

**Analysis of the proteome of red and green leaf phenotypes of  
'Bon Rouge' pear trees *Pyrus communis* L. by 2-dimensional  
gel electrophoresis**

Majimi James Sehata

A thesis submitted in partial fulfilment of the requirements for the  
degree of Magister Scientiae in the Faculty of Sciences, University  
of the Western Cape

The logo of the University of the Western Cape, featuring a classical building facade with columns and a pediment, positioned above the text 'UNIVERSITY of the WESTERN CAPE'.

UNIVERSITY of the  
WESTERN CAPE

Supervisor: Marlene du Preez

Co-supervisors: Bongani Ndimba

Jasper Rees

November 2007

**Analysis of the proteome of red and green leaf phenotypes of ‘Bon Rouge’ pear trees**

***Pyrus communis* L. by 2-dimensional gel electrophoresis**

Majimi James Sehata

**KEYWORDS**

Proteomics

SDS-PAGE

2D-PAGE

‘Bon Rouge’

‘Bon Rouge’ revertants

Anthocyanins

Proteins

RuBisCO

IEF

MALDI-TOF



UNIVERSITY *of the*  
WESTERN CAPE

## ABSTRACT

### **Analysis of the proteome of red and green leaf phenotypes of ‘Bon Rouge’ pear trees *Pyrus communis* L. by 2-dimensional gel electrophoresis**

M. J. Sehata

MSc Thesis, Department of Biotechnology, Faculty of Natural Science, University of the Western Cape.

The ‘Bon Rouge’ pear is a red pear cultivar derived from a rare, spontaneous bud mutation which occurred on the green pear ‘William’s Bon Chretien’ (Bartlett). ‘Bon Rouge’ pear cultivar was observed to be reverting back to its original phenotypic green colour. To study the cellular changes occurring within the cells both the mutated red phenotype and the wild type green phenotype of ‘Bon Rouge’ were investigated using proteomics approach. The proteins from the tissues of interest were precipitated in the presence of 10% TCA and solubilized in urea/thiourea lysis buffer. The proteins were separated on 12% SDS-PAGE and 2D PAGE in order to compare their protein expression profiles. The results from SDS-PAGE and 2D PAGE profiles show an elevated level of 53 kDa protein in green pears which was either absent or less expressed in red phenotype and this protein appears to be the only differentiating factor between the red and green ‘Bon Rouge’ phenotypes. This protein was subsequently identified by the MALDI-TOF-MS to be large subunit of RuBisCO. Expression proteomics is a preferred method due to its reproducibility and it has a potential to provide direct identification of cultivars related

proteins. Additionally, proteomics approaches could help the fruit crop growers and breeders, to select and determine types of different cultivars at various growth stages.



UNIVERSITY *of the*  
WESTERN CAPE

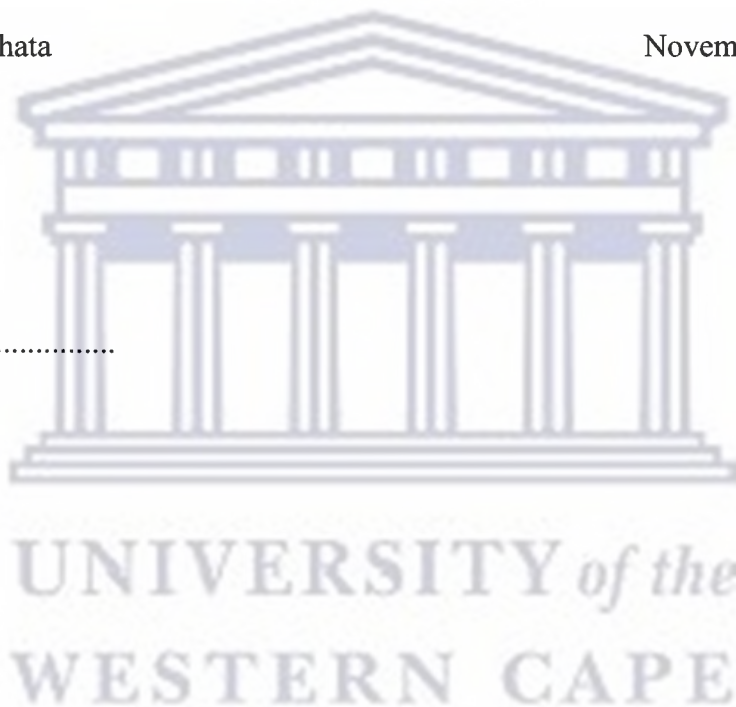
## DECLARATION

I declare that *Analysis of the proteome of red and green leaf phenotypes of 'Bon Rouge' pear trees Pyrus communis L. by 2-dimensional gel electrophoresis* is my own work, that it has not been submitted for any degree or examination in any other university, and that all the sources I have used or quoted have been indicated and acknowledge by complete references.

Majimi James Sehata

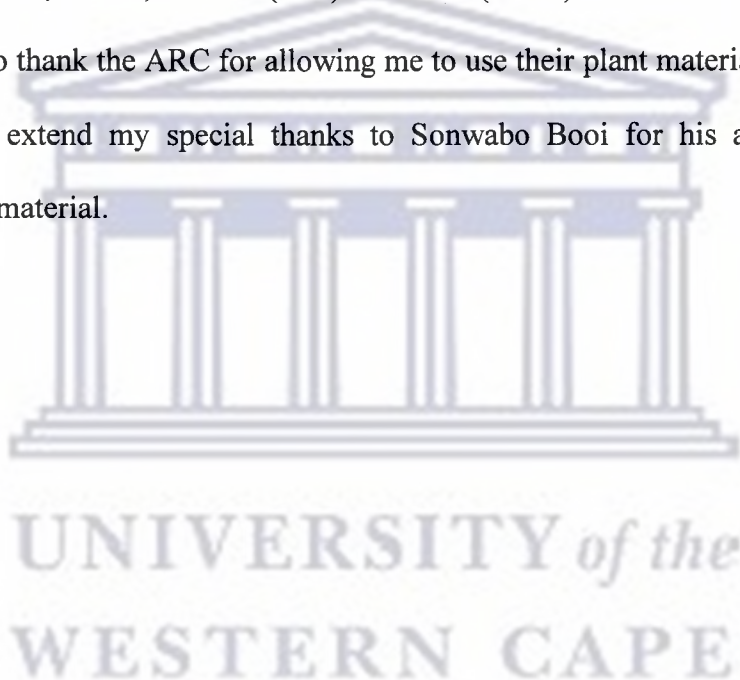
November 2007

Signed.....



## ACKNOWLEDGEMENTS

I would like to thank the almighty God for making everything possible for me in my studies, without him it would not have been possible. I am also grateful to my supervisors Marlene du Preez, Bongani Ndimba and Jasper Rees for the opportunity they gave me to join their research group and for all their assistance regarding my research project. I'm also thankful to the entire Proteomics research group lab members (Rudo, Xoli, Nonku, Morleen and Simpiwe) for all their valuable inputs during the construction of my thesis. I am thankful to NRF, DFPT, THRIP (DTI) and SNS (UWC) for financial support and I would also like to thank the ARC for allowing me to use their plant material, in particular I would like to extend my special thanks to Sonwabo Booï for his assistance with sampling of leaf material.



## LIST OF TABLES

<b>Table 1.1</b> European pears ( <i>Pyrus cummunis</i> L.) production in Africa versus the world productions from the period 1998-2002	4
<b>Table 1.2</b> Comparison of selected South African fruit tree statistics in hectares and percentages	5
<b>Table 1.3</b> Pear cultivars distributions (hectares) in South Africa	6
<b>Table 1.4</b> Pear cultivar export volumes in South Africa	7
<b>Table 2.1</b> Plant leaf material from pear trees	33
<b>Table 2.2</b> Chemicals	34
<b>Table 2.3</b> Preparation of BSA standard solutions for Bradford Assay for generation of a standard curve	40
<b>Table 2.4</b> Protein quantification of the pear plant tissues	40
<b>Table 3.1</b> Average protein concentration from pear tissues	48
<b>Table 4.1</b> Summary of all spots identified by MALDI-TOF	67



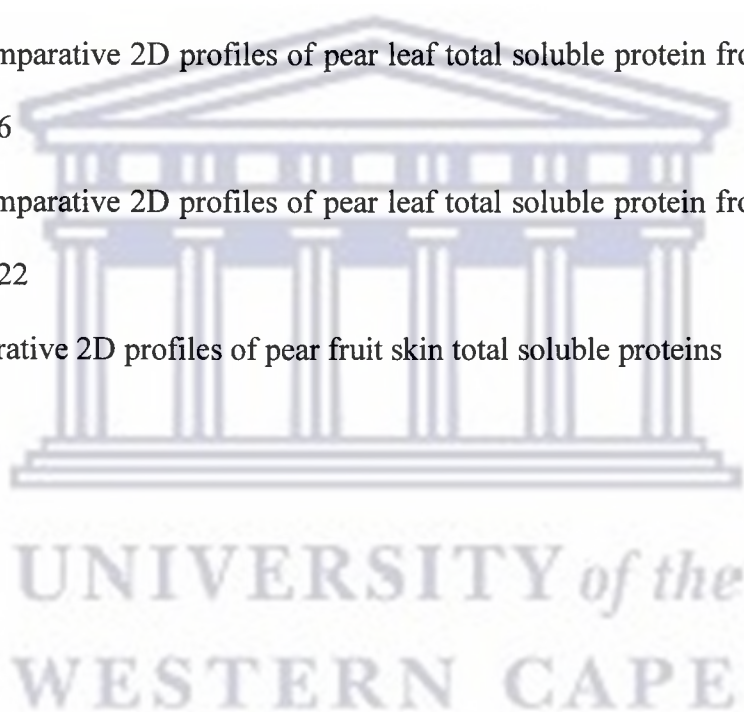
UNIVERSITY of the  
WESTERN CAPE

## LIST OF FIGURES

<b>Figure 1.1</b> Examples of members of pome fruit crops	2
<b>Figure 1.2</b> ‘Bon Rouge’ pear fruits and seedlings	9
<b>Figure 1.3</b> Schematic diagram of biotic stresses effects	12
<b>Figure 1.4</b> General structure of anthocyanins	21
<b>Figure 1.5</b> General anthocyanin biosynthesis pathway	22
<b>Figure 1.6</b> Number of articles using the term proteomics	27
<b>Figure 1.7</b> Overview of common steps involved in protein identification	29
<b>Figure 3.1</b> 1D SDS-PAGE profiles of total soluble proteins from pear tissue	49
<b>Figure 3.2</b> 2D profiles showing poor gel resolution	53
<b>Figure 3.3</b> Established proteome maps of total soluble proteins from pear tissue	54
<b>Figure 4.1</b> 1D SDS-PAGE profiles of pear leaf total soluble proteins	61
<b>Figure 4.2</b> 1D SDS-PAGE profiles of pear leaf total soluble proteins	62
<b>Figure 4.3</b> Comparative 2D profiles of ‘Bon Rouge’ and ‘Bon Rouge’ revertant using their total soluble proteins	63
<b>Figure 4.4A</b> MALDI-TOF-MS data from the tryptic digest of protein spot 7 from ‘Bon Rouge’ leaf	66



<b>Figure 4.5.1</b> Comparative 2D profiles of pear leaf total soluble proteins from pear clones BR1 and BRR1	69
<b>Figure 4.5.2</b> Comparative 2D profiles of pear leaf total soluble protein from pear clones BR7 and BRR7	70
<b>Figure 4.5.3</b> Comparative 2D profiles of pear leaf total soluble protein from pear clones BR8 and BRR8	71
<b>Figure 4.5.4</b> Comparative 2D profiles of pear leaf total soluble protein from pear clones BR9 and BRR9	72
<b>Figure 4.5.5</b> Comparative 2D profiles of pear leaf total soluble protein from pear clones BR16 and BRR16	73
<b>Figure 4.5.6</b> Comparative 2D profiles of pear leaf total soluble protein from pear clones BR 22 and BRR 22	74
<b>Figure 6</b> Comparative 2D profiles of pear fruit skin total soluble proteins	75



## LIST OF ABBREVIATIONS

1D PAGE	One-dimensional gel electrophoresis
2D PAGE	Two-dimensional gel electrophoresis
3GT	Flavonoid 3- <i>O</i> -glucosyltransferase
ANS	Anthocyanidin synthase
APS	Ammonium Persulphate
BLAST	Basic local alignment search tool
BR	'Bon Rouge'
BRR	'Bon Rouge' revertant
BSA	Bovine serum albumin
CHAPS	3-[(3-Cholamidopropyl) dimethylammonio]- 1-propanesulfonate
CBB	Coomassie Brilliant blue
cm	Centimetre
CO <sub>2</sub>	Carbon dioxide
CS	Chalcone synthase
DHK	dihydrokaempferol
DTT	Dithiothreitol
<i>et al</i>	et alibi
F3H	Flavanone 3-hydroxylase
Ha	Hectare
IEF	Isoelectric focusing

IPG	Immobilized pH gradient
kDa	Kilo Daltons
kVh	Kilo Volt-hours
M	Molar
m/z	mass per charge
MALDI-TOF	Matrix assisted laser desorption ionisation time of flight
ml	Millilitre
mm	Millimetre
mM	Millimolar
MOWSE	Molecular weight search
MSDB	Mass spectrometry database
NI	Not identified
PAL	Phenylalanine ammonia-lyase
pI	Isoelectric point.
SDS	Sodium dodecyl sulfate
SDS-PAGE	Sodium dodecyl sulfate polyacrylamide gel electrophoresis
TCA	Trichloroacetic acid
TEMED	N, N, N <sup>1</sup> ,N <sup>1</sup> - Tetra methylethelene-diamine
TFA	Trifluoroacetic acid
TSP	Total soluble protein
µg	Microgram

$\mu\text{g}/\mu\text{l}$	Microgram per microlitre
$\mu\text{l}$	Microlitre
UV	Ultraviolet
V	Volts
v/v	Volume per volume
w/v	Weight per volume



UNIVERSITY *of the*  
WESTERN CAPE

## TABLE OF CONTENTS

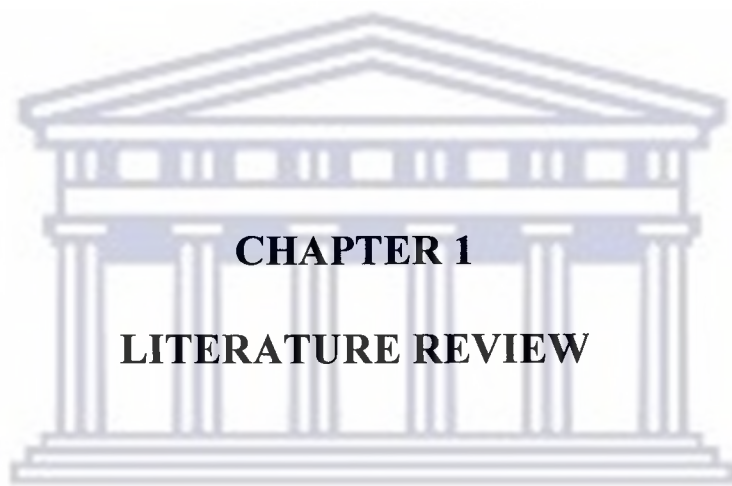
TITLE.....	i
KEYWORDS.....	ii
ABSTRACT.....	iii
DECLARATION.....	v
ACKNOWLEDGEMENTS.....	vi
LIST OF TABLES.....	vii
LIST OF FIGURES.....	viii
ABBREVIATIONS.....	x
<b>CHAPTER 1: LITERATURE REVIEW.....</b>	<b>1</b>
1.1 Introduction.....	2
1.2 Taxonomy of pears.....	2
1.3 Status of pear production in Africa.....	3
1.4 Commercial uses of pears.....	5
1.5 Different skin colours of pear fruits.....	7
1.5.1 The ‘Bon Rouge’ pear.....	8
1.6 Plant stresses.....	10
1.6.1 Abiotic stress.....	10
1.6.1.1 Salt stress.....	10
1.6.2 Biotic stress.....	11
1.7 Plants response to environmental stress.....	13

1.8 Environmental regulation of colour development in fruit.....	14
1.8.1 Light.....	14
1.8.2. Temperature.....	14
1.8.2.1 Cold temperature induction.....	15
1.8.3 Nutrient deficiency induction.....	15
1.9 Plant pigments.....	16
1.9.1 Anthocyanins.....	16
1.9.1.1 Anthocyanin biosynthesis.....	17
1.10 Anthocyanin biosynthesis via the shikimic acid pathway	18
1.10.1 Phenylalanine ammonia-lyase (PAL).....	18
1.10.2 Cinnamic acid 4-hydrolase.....	19
1.10.3 Anthocyanidin synthase (ANS).....	19
1.10.4 Flavonoid 3- <i>O</i> -glucosyl transferase (3GT).....	20
1.11 Role of bHLH and MYC in anthocyanin synthesis.....	20
1.12 Degradation of anthocyanins.....	23
1.13 Properties of anthocyanin in plants.....	23
1.13.1 Anthocyanins as sunscreens.....	24
1.13.2 Anthocyanins as antioxidants.....	25
1.13.3 Biological activities of anthocyanins.....	25
1.14 From genomics to proteomics.....	25

1.14.1 Plant proteomics.....	26
1.14.2 Where the strength of proteomics lies.....	27
1.15 Gel visualization.....	30
1.15.1 Coomassie brilliant blue.....	30
1.15.2 SYPRO Ruby.....	30
1.16 Principles of and instrumentation in mass spectrometry.....	30
1.17 Objectives of this study.....	32
<b>CHAPTER 2: MATERIALS AND METHODS.....</b>	<b>33</b>
2.1 Materials.....	34
2.1.1 Pear leaf material.....	34
2.1.2 Pear Fruit material.....	35
2.1.3 Sampling, delivery and storage of pear material.....	35
2.1.4 Chemicals list.....	35
2.1.5 General stock solutions and buffers used.....	37
2.2 Methods.....	39
2.2.1 Protein extraction.....	39
2.2.1.1 Protein extraction from pear leaves.....	39
2.2.1.2 Protein extraction from pear fruit.....	39
2.2.2 Protein quantification.....	40
2.2.3 1D SDS-PAGE.....	42
2.2.4 Staining of the gels.....	42
2.2.5 Second dimensional gel preparation.....	43
2.2.5.1 Reswelling of IPG strips.....	43

2.2.5.2 Isoelectric focusing (IEF) of IPG strips.....	43
2.2.6 In-gel digestion of protein spots from 2D gels.....	44
<b>CHAPTER 3: ESTABLISHMENT OF PROTEOME MAPS.....</b>	<b>46</b>
3.1 Introduction.....	47
3.2 Results and discussion.....	47
3.2.1 Optimization of protein extraction and 1D SDS-PAGE.....	47
3.2.2 Establishment of 2D PAGE proteome maps of pear tissues.....	51
3.4 Summary.....	56
<b>CHAPTER 4: COMPARISON OF RED AND GREEN ‘BON ROUGE’ PHENOTYPES AND PROTEIN IDENTIFICATION.....</b>	<b>57</b>
4.1 Introduction.....	58
4.2 Results and discussion.....	59
4.2.1 1D SDS-PAGE of red and green ‘Bon Rouge’ phenotypes using total Soluble proteins (TSP).....	59
4.2.2 2D-PAGE of the red and green ‘Bon Rouge’ phenotypes.....	61
4.2.3 Protein identification.....	65
4.3 Comparative analysis of protein profiles of pear leaf clones and fruit skins.....	69
4.4 Summary.....	77
<b>CHAPTER 5 GENERAL DISCUSSION AND FUTURE WORK.....</b>	<b>78</b>
<b>CHAPTER 6: REFERENCES.....</b>	<b>83</b>





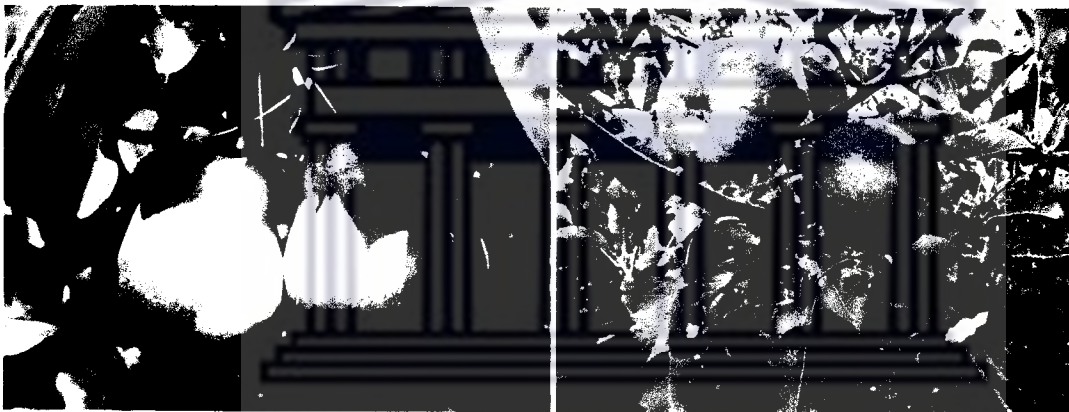
**CHAPTER 1**

**LITERATURE REVIEW**

UNIVERSITY *of the*  
WESTERN CAPE

## 1.1 Introduction

Pome fruit belong to the Rosaceae or rose family, subfamily Pomoideae (Figure 1.1). Pome fruit is an economic-botanical plant group that includes a large number of species and cultivars, particularly diverse for apples and pears. The most important species for fruit growing are apples, pears and quinces. In comparison with other fruit crops, pomes are distinguished by their high winter cold tolerance and longevity. Propagation of the fruit is done typically by grafting suckers and cuttings onto suitable rootstock. Fruits of many pome plants, in contrast to those of stone and small fruits, can be kept fresh for a long time (Dzhangaliev *et al.*, 2003).



**A** **B**  
**Figure 1.1:** Examples of members of pome fruit crops. (A) Pear fruits and (B) Apples fruits.

## 1.2 Taxonomy of pears

Pears are the third most important fruit produced in temperate regions after grapes and apples. They belong to the genus *Pyrus*, which comprises at least twenty-two species of which the European pear *P. communis* L., and *P. pyrifolia* are the most interesting for fruit production. Both are diploid and self-incompatible, and there is a great genetic variability within their species (Oliveira *et al.*, 1999). Among the twenty-two primary species that belong to the genus *Pyrus*, *P. communis* L. is wide-spread throughout Europe, North and South America, Africa and Australia while *P. pyrifolia* is mainly cultivated in Southern and

Central China and Japan (Monte-Corvo *et al.*, 2000). The common pear, *Pyrus communis* L., is also referred to occasionally as *P. communis* var *pyraster* L. or *P. pyraster* (L.) Burgsd. The wild native trees are deciduous and grow to a height of up to almost 20 m. The branches form short stiff spurs, which are sometimes spiny. The leaves of the common pear are somewhat variable from ovate heart-shaped and oval to almost round between 2.5 and 10 cm in length and approximately 5 cm wide. Some have finely-toothed margins while others are entirely smooth. Flowers are white, 2.5 to 3.75 cm in diameter and are produced in corymbs of 5 to 7.5 cm across each flower on a stalk of around 1 to 3 cm in length. The fruits are typical pear shaped with a tapering or rounded base (Tromp *et al.*, 2005).

Very few cultivars of *P. communis* L. satisfy standards for fruit quality and clonal fidelity; thus, accurate verification of cultivar identity for checking propagation material and patent protection is very important. Traditional methods for testing genetic variability in fruit crops were based on morphological or time-consuming physiological assays (Schiliro *et al.*, 2001). Recently, some biochemical markers like isozymes provided useful information but these still have some disadvantages such as the limited number of polymorphisms detected between close genotypes, and variations due to physiological stages (Oliveira *et al.*, 1999).

### **1.3 Status of pear production in Africa**

In the context of global production, Africa is the smallest producer of European pears (*P. communis* L.) with roughly 3% of global plantings and production as shown in Table 1.1. On the African continent, South Africa is by far the largest producer, with 56% of the total production. It is followed by Algeria (16%), Tunisia (11%), Egypt (9%) and Morocco (8%) respectively. On the other hand Madagascar, Libya, Zimbabwe and Kenya combined, total to less than 1% of the continent's production (Ferrandi *et al.*, 2005).

**Table 1.1** European pear (*Pyrus communis* L.) production in Africa versus the world production from the period 1998-2002 (Ferrandi *et al.*, 2005).

Year	Hectares		Production (tonnes)	
	World	Africa	World	Africa
1998	1 487 516	43 674	15 223 755	441 701
1999	1 540 839	46 024	15 657 212	513 065
2000	1 594 699	46 995	16 756 405	477 649
2001	1 591 588	47 616	16 707 008	477 651
2002	1 780 473	48 322	17 115 205	530 547

Therefore, the pear industry, is the third largest in the South African fruit industry, and is very important in terms of size, export and economic impact. A total of 76 676 ha under deciduous fruits production, 12 912 ha are devoted to pear production as shown in Table 1.2 (Human, 2005). During the 2001/2002 season, the pear industry exported 8 095 817 standard cartons with a value of R580 193 000 (Human, 2005). A summary of cultivars and export figures for the pear industry is shown in Table 1.3 and Table 1.4 respectively. Pears are planted in most of the deciduous fruit producing areas of South Africa, with Ceres being the most important production region in the Western Cape. Imported cultivars are usually poorly adapted to South African conditions, mainly because they require more cold units than are locally available. Thus, in order to remain competitive on overseas markets, the South African pear industry must therefore generate, through breeding programs, an ongoing supply of climatically adapted cultivars (Human, 2005).

**Table 1.2** Comparison of selected South African fruit tree statistics in hectares and percentages (Human, 2005).

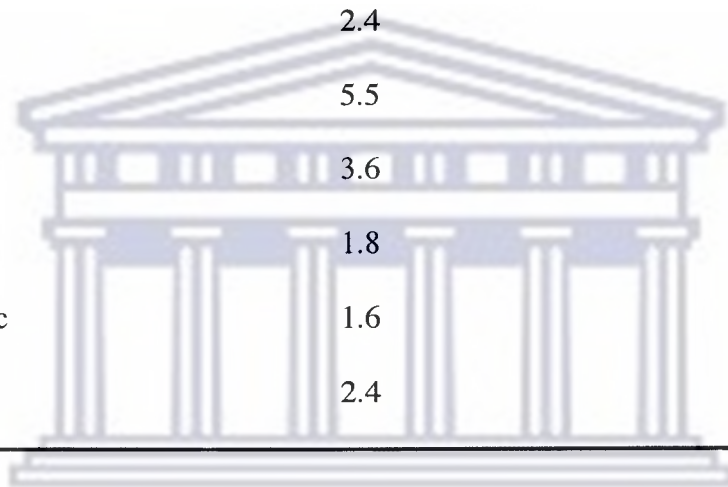
<b>Fruit kind</b>	<b>Ha</b>	<b>% of the total plantings</b>
Apples	22 454	29.3
Grapes	20 643	26.9
Pears	12 912	16.8
Apricots	4 751	12.5
Plums	4 962	6.5
Nectarines	1 379	1.8

#### **1.4 Commercial uses of pears**

Large amounts of the fruits of common pears produced worldwide are consumed fresh. Whilst some of these fruits must be consumed within just a few weeks of harvesting, a large proportion of what is commonly known as “winter pears,” can tolerate storage under controlled atmospheric conditions for many months. Large quantities of common pear fruits are exported from major areas of production to other consuming countries and are moved in large quantities between hemispheres (Tromp *et al.*, 2005). Many of the common pears produced are also processed and significant quantities of their cultivars such as ‘Williams’ are grown for canning. Pears are also used in the production of alcoholic and other beverages (Tromp *et al.*, 2005). Specific cultivars of pears, mostly those that have *P. nivalis* in their parentage, are used to produce Perry, a high quality alcoholic drink with “champagne” type properties. Pear fruits are also used, especially in mid and Eastern European countries, to produce a distilled spirit drink known as brandy (Tromp *et al.*, 2005).

**Table 1.3** Pear cultivars distributions (hectares) in South Africa (Human, 2005).

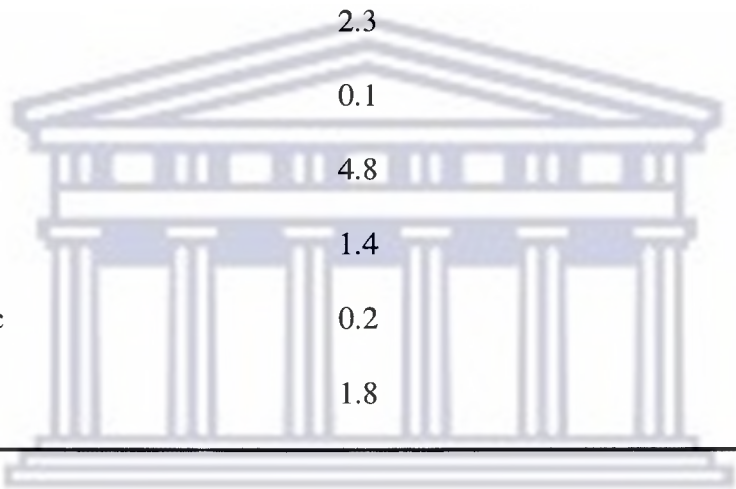
<b>Cultivar</b>	<b>Ha (%)</b>
Packham's Triumph	28.0
Bon Chretien	25.1
Forelle	15.8
Beurre Bosc	5.0
Rosemarie	5.5
Doyenne Du Comice	3.3
Beurre Hardy	2.4
Early Bon Chretien	5.5
Flamingo	3.6
'Bon Rouge'	1.8
Golden Russet Bosc	1.6
Other	2.4



UNIVERSITY *of the*  
WESTERN CAPE

**Table 1.4** Pear cultivar export volumes in South Africa (Human, 2005).

<b>Cultivar</b>	<b>Cartoons (%)</b>
Packham's Triumph	53.2
Bon Chretien	15.9
Forelle	11.4
Beurre Bosc	5.0
Rosemarie	4.8
Doyenne Du Comice	2.6
Beurre Hardy	2.3
Abate Fetel	0.1
Flamingo	4.8
'Bon Rouge'	1.4
Golden Russet Bosc	0.2
Other	1.8



### **1.5 Various skin colours of pear fruits**

The skin of pears grows in a broad array of colours such as green, yellow, orange and red that act as deterrents from attack by birds and other animals (Malcolm, 2006). This colouring is necessary because pear trees require longer periods of maturity to begin fruiting than most other fruit trees, but the tree will bear fruits earlier if grafted on a dwarfing quince rootstock (Malcolm, 2006). Pear fruits contain antioxidants and no fats, with health benefits from vitamins A, B<sub>1</sub>, B<sub>2</sub>, C, niacin and the minerals calcium, phosphorus, iron and potassium (Malcolm, 2006). There is a need to guide the horticultural development of new products, since without access to taste information, consumers are forced to make decisions based on the way the product looks. Appearance of fruits in the market place is of critical importance to consumers, often setting up expectation of what the product will taste like. As a result

decisions to commercialize an advance selection from a fruit-breeding program also need to be cognisant of the impact of shape, colour and appearance on consumer acceptance of the product (Gamble *et al.*, 2006).

### 1.5.1 'Bon Rouge' pears

'Bon Rouge' pears are characterized by red skinned fruit (Figure 1.2A) throughout the growing season and red leaves early in the season (Figure 1.2B). This pear cultivar was developed from a bud mutation that arose spontaneously on a William's Bon Chretien (Bartlett) pear tree (du Preez and Rees, 2005). The 'Bon Rouge' pear trees show a high level of reversion to the parent phenotype that manifest itself as red and green sectors on leaves and fruit skin (Figure 1.2C), or completely green leaves (Figure 1.2D) and fruit skin (Figure 1.2E) (Booi *et al.*, 2005). Red and blushed pears acquire their red colour from anthocyanins present in their peel (Steyn *et al.*, 2004). Blushed pear fruits are sought after by consumers and fetch higher prices than green or fully red fruits (Steyn *et al.*, 2005).



UNIVERSITY of the  
WESTERN CAPE



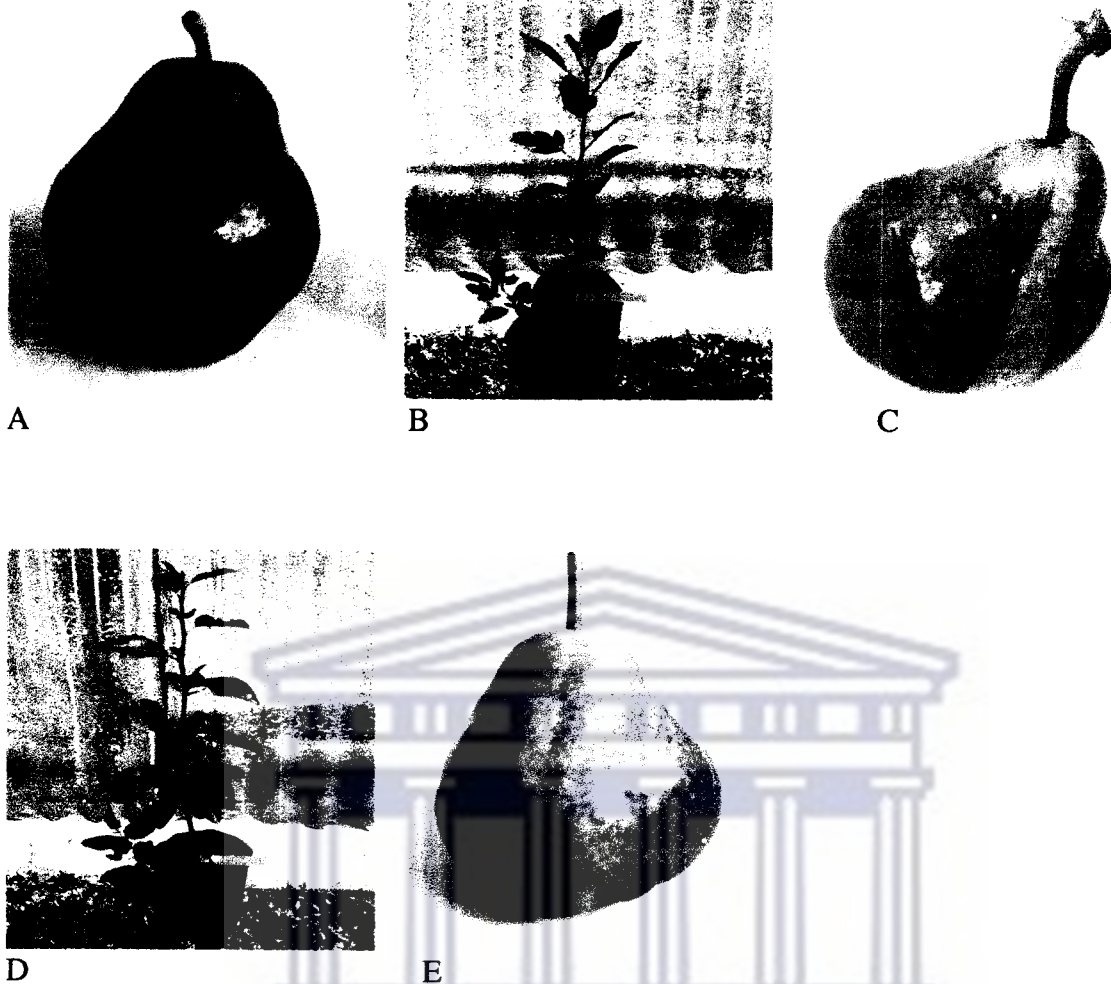


**Figure 1.2:** 'Bon Rouge' pear fruits and seedlings. (A) 'Bon Rouge' pear fruit, (B) 'Bon Rouge' seedling with red coloured leaves, (C) 'Bon Rouge' pear fruit with revertant sectors, (D) 'Bon Rouge' revertant seedling with complete reverted green leaves and (E) 'Bon Rouge' revertant pear fruit.

The red colour of blushed fruit is due to the presence of two anthocyanin pigments, cyanidin 3-galactoside and cyanidin 3-arabinoside, that are found in the hypodermal layers of the skin (Steyn *et al.*, 2005; Ubi, 2004; Ubi *et al.*, 2006). The presence and the extent of the red blush, which varies considerably between seasons and between cultivars, determines the profitability of blushed cultivars. Differences in the redness of pear peel primarily relate to the differences in pigment levels. Hence, poor red colour and downgrading of blushed pears is normally attributed to low anthocyanin levels at harvest. In order to attain regular yields of

sufficiently blushed fruits, producers need to be aware of the factors that influence pear red colour development (Steyn *et al.*, 2005).

## **1.6 Plant stresses**

Plants are frequently exposed to stress factors. These are generally defined as external conditions that may adversely affect growth, development, or productivity of the plant. Any unfavourable condition or substance that affects or blocks a plant's metabolism, growth or development can be regarded as stress. Stress can either be biotic (imposed by other organisms) or abiotic (arising from an excess or deficit in the physical or chemical environment) (Munne-Bosch and Alegre, 2004).

### **1.6.1 Abiotic stress**

Abiotic stresses, such as a drought, salinity, extreme temperature and chemical toxicity are serious threats to agriculture and can result into the deterioration of the environment (Wang *et al.*, 2003). Abiotic stress is the primary cause of crop losses worldwide, reducing average yields of most major crop plants by more than 50% (Wang *et al.*, 2003). Abiotic stress leads to a series of morphological, physiological, biochemical and molecular changes that adversely affect plant growth and productivity (Wang *et al.*, 2003).

#### **1.6.1.1 Salt stress**

Understanding the mechanisms of salt tolerance in plants is increasingly important as soil salinity is becoming a greater problem in countries where agricultural land is dependant on irrigation. A high concentration of salt in the soil solution has adverse effects on plants because of reduced water potential, specific ion stress or toxicity, and ion imbalance or nutrient deficiency, all of which can cause reduced growth and decreased crop productivity.

Worldwide, approximately 230 million hectares are currently under irrigation and one-third of this number is affected by salinity (Katterman, 1990). Attempts to alleviate the progressive salt build-ups in crop lands include the implementation of reclamation, drainage, and irrigation practices that minimize the salinity levels to which crops are exposed. However, even with this highly sophisticated agrotechnology, increasing soil salinity still remains a major problem (Katterman, 1990).

A need for some costly engineering solutions to combat the problem of salinity may be reduced by the development of plants that are more salt tolerant. However, most of the crop plants have relatively low salt tolerance levels. In order to develop salt tolerance crops, it is important to understand the mechanism that plants use to cope with a saline environment and still maintaining productivity. This entails understanding the effects of salt at the physiological, biochemical, and molecular levels (Katterman, 1990).

One approach in studying the mechanisms involved in salt tolerance is to use two-dimensional polyacrylamide gel electrophoresis (2D-PAGE) to identify polypeptides whose levels increase in salt-tolerant plants in response to salt stress. The assumption is that these polypeptides have a role in the plant's adaptation to salt stress. Protein synthesis responds dramatically to environmental stresses such as heat shock, where the synthesis of most proteins ceases and the synthesis of a new set of proteins is induced (Katterman, 1990).

### **1.6.2 Biotic stress**

During their life cycle, plants are exposed to invading microorganisms, including bacteria, fungi, filamentous protist oomycetes, and viruses that are potentially pathogenic. These pathogenic organisms impair host plant growth. As sessile organisms without mobile sentry

cells, plants must respond to such potentially injurious microbe invasion using defence strategies that include chemotaxis-facilitated phagocytosis (Ma and Berkowitz, 2007). Thus, attacks on the root system can induce changes in the shoot and vice versa (Bruce and Pickett, 2007). Plants share with animals the use of  $\text{Ca}^{2+}$  as a cytosolic secondary messenger molecule involved in numerous cell signalling cascades responding to abiotic and biotic stimuli (Figure 1.3) (Ma and Berkowitz, 2007).

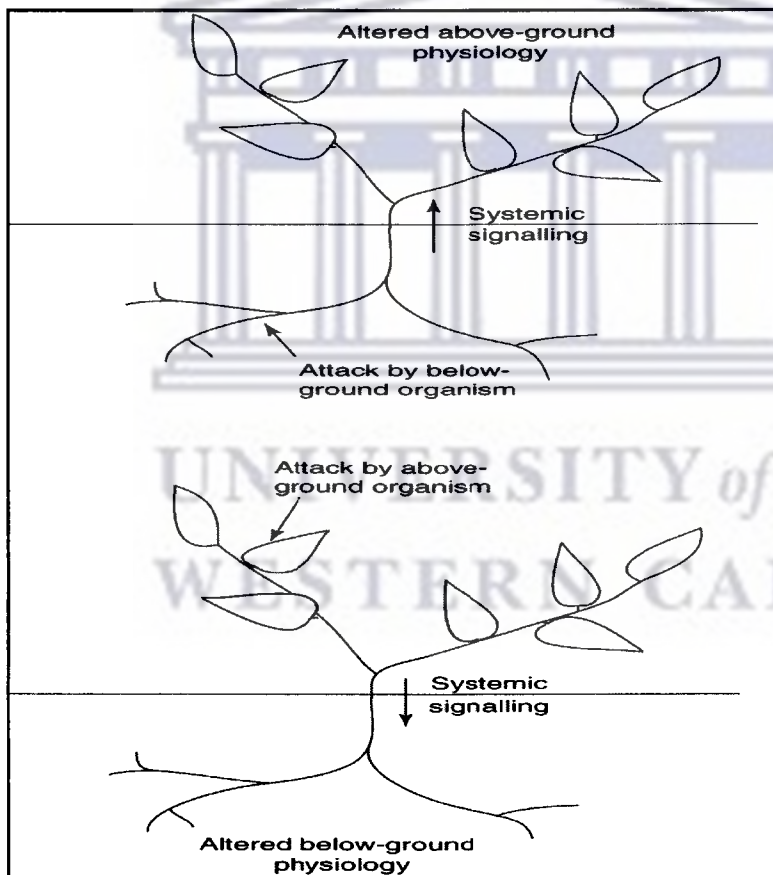


**Figure 1.3:** Schematic diagram of biotic stresses effects (Bruce and Pickett, 2007).

## 1.7 Plant response to environmental stress

Anthocyanins accumulate when either environmental or developmental changes render plants more sensitive to the environment. The ability to induce anthocyanin accumulation may sometimes be limited to the juvenile phase, or lost with increasing age and reduced sensitivity to environmental stress (Steyn *et al.*, 2002). Anthocyanins often appear transiently at specific developmental stages and may be induced by a number of environmental factors that include visible and ultraviolet (UV-B) radiation, cold temperature and water stress (Chalker-Scott, 1999). The UV-absorbing characteristics of flavonoids have long been considered to be evidence for the role of flavonoids in UV protection. The flavonoids are often present in the epidermal cell layers of leaves and in tissues that are susceptible to UV light, such as pollen and the apical meristems (Winkel-Shirley, 2002). The subsequent production and localisation of the anthocyanins in roots, stems and especially leaf tissues may allow a plant to develop resistance to a number of environmental stresses (Chalker-Scott, 1999). Apart from their widely reported distribution in floral tissues, anthocyanins are also located in the roots, shoots and leaves. The presence of anthocyanin has been reported in the root cap of 'Impatiens' seedlings and in roots under osmotic or toxin stress. Stems may accumulate anthocyanins, often as a function of juvenility, osmotic stress or cold temperature shock (Chalker-Scott, 1999).

In general, anthocyanins are believed to increase the antioxidant response of plants in order to uphold the regular physiological status in tissues that are directly or indirectly affected by biotic and abiotic stress factors (Stintzing and Carle, 2004). This property is best exemplified by the juvenile reddening which is a temporary event of high metabolic activity (Stintzing and Carle, 2004). Although mainly reported for vegetative tissues, it is very likely that anthocyanins fulfil the same task in reproductive plant parts (Stintzing and Carle, 2004).

## **1.8 Environmental regulation of colour development in fruits**

The stimulation of anthocyanin biosynthesis in plants can be influenced by many factors such as light, temperature, phytohormones, sugar and the presence of iron (Lu and Yang, 2006).

### **1.8.1 Light**

Light is one of the main determinants of anthocyanin production in fruits and their biosynthesis is dependent on light intensity (Merzlyak and Chivkunova, 2000). Generally, apples do not redden when kept under low light or dark treatment. The requirement for light is evident from the usual reduction in red colour development on the skin, a phenomenon naturally observed in the interior of a tree canopy (Ubi, 2004). The biosynthesis of anthocyanins in maturing fruits is therefore a light dependent process. The effect of light on anthocyanin biosynthesis is generally attributed to a requirement for a photomorphogenic signal, mediated by photoreceptors or to a shortage of carbohydrates caused by restricted photosynthesis under low light conditions (Ubi, 2004). Carbohydrates can play two roles in anthocyanin biosynthesis by providing the substrate for flavanoid biosynthesis via shikimic acid and phenylpropanoid pathways, and as an inducer of genes involved in anthocyanin biosynthesis (Ubi, 2004).

### **1.8.2 Temperature**

Temperature has a profound effect on anthocyanin production in fruits. Low temperatures, such as those encountered during cold nights, enhance anthocyanin synthesis, and high temperature inhibits anthocyanin accumulation in apple fruit skin (Ubi, 2004). The effect of low temperature has been suggested to arise from a reduction in loss of sugars from the skin through respiration, resulting in increased photosynthate levels, which would then flow through to the anthocyanin biosynthesis (Ubi, 2004).

### **1.8.2.1 Cold temperature induction**

Induction of anthocyanin biosynthesis by cold temperature has received less attention than photoinduction, even though the evidence for this process is seen in deciduous plants every fall. Low temperature has been shown to induce anthocyanin synthesis in the seedlings of *Arabidopsis*, sorghum and *Z. mays* (Chalker-Scott, 1999). Anthocyanins, acting as light screening pigments, are believed to accumulate in leaves and stems in response to low temperature and changes in light. Phenylalanine ammonia-lyase (PAL) activity has also been shown to increase in response to low temperature in different species. Furthermore, a correlation between low temperature-induced anthocyanin synthesis and accumulation of PAL and Chalcone synthase (CHS) mRNA has been demonstrated in maize (Leyva *et al.*, 1995).

### **1.8.3 Nutrient deficiency induction**

Accumulation of anthocyanin is also associated with macronutrient deficiencies, particularly in intensively-managed agricultural, horticultural, or forest productions where the nutrients contained in produce are removed from the system and replaced through fertilizer application (Close and Beadle, 2003).

Nutrition and particularly nitrogen (N) deficiency detrimentally affects photosynthetic function and efficiency, and decreases the levels of Calvin Cycle enzymes. This effect commonly induces or enhances the accumulation of anthocyanins in leaves of many plant species (Close and Beadle, 2003). Phosphorus (P) deficiency, which restricts phosphate levels for energy metabolism, also increases anthocyanin content in a range of monocotyledonous and dicotyledonous plants (Close and Beadle, 2003).

## 1.9 Plant pigments

Colour development of flowers and fruit is an important evolutionary trait in plant fitness. Plant colour is a blend of chlorophyll, carotenoids and flavonoids. Flavonoids can act as UV and pathogen protectants as well as signal molecules in the interaction between plants and bacteria. Anthocyanin, a sub-class of flavonoids, has been implicated as a major colour pigment in plants. The yellow and green background colour in fruits is due to chlorophylls and carotenoids stored in the plastids, whereas the red colour is produced mainly by anthocyanins in the vacuoles of epidermal cells (Kim *et al.*, 2003).

The distribution of anthocyanins within organs and tissues is genetically determined by tissue-specific expression of regulatory genes. These genes control the expression of structural genes in response to environmental and developmental cues (Steyn *et al.*, 2002). Anthocyanin synthesis is a cell-autonomous response, meaning that colour development is controlled at the level of individual cells (Steyn *et al.*, 2002).

### 1.9.1 Anthocyanins

Anthocyanins are water-soluble pigment found in all plant tissues throughout the plant kingdom. They give colour to fruits and autumn leaves (Chalker-Scott, 1999). Anthocyanins are pigments that only occur in the cytoplasm of land plants but not animals, microorganisms or waterplants. The reason for this is that anthocyanin biosynthesis requires some chemical starting materials that are derived from plant photosynthesis. In waterplants, the light intensity under water is not sufficient for this production (Sullivan, 1998). Anthocyanins belong to a widespread class of phenolic compounds collectively named flavonoids (Kong *et al.*, 2003; Robinson and Robinson, 1931; Sass-Kiss *et al.*, 2005). The anthocyanins themselves are



subdivided into sugar-free anthocyanidin aglycons and anthocyanin glycosides (Feild *et al.*, 2001).

Anthocyanin accumulation in grapes begins at veraison, the onset of ripening. Their accumulation is enhanced by a plant hormone, abscisic acid (ABA), and suppressed by synthetic auxins, high temperature and low light intensity (Jeong *et al.*, 2004).

### 1.9.1.1 Anthocyanin biosynthesis

Two groups of genes are required for anthocyanin biosynthesis; the structural genes encoding the enzymes directly implicated in the biosynthesis reactions, and the regulatory genes encoding the transcription factors which control the expression of the above-mentioned structural genes (Lo Piero *et al.*, 2005; Holton and Cornish, 1995). Therefore, loss of anthocyanin synthesis can arise by mutations in individual structural genes, or by alteration of regulatory genes controlling the expression of a number of the structural genes (Lo Piero *et al.*, 2005). Moreover, anthocyanin production may be induced by a number of environmental factors including visible and UVB radiation, cold temperature, water stress and low phosphorus content in the soil (Lo Piero *et al.*, 2005). On the other hand, anthocyanin accumulation can be induced in mature green leaves by various biotic or abiotic stresses like wounding, pathogen attack and nutrient deficiency (Manetas, 2005).

The committing step for anthocyanin biosynthesis involves an enzyme, called chalcone synthase (CS), which catalyses the step-wise condensation of three malonyl-CoA units with p-coumaroyl-CoA to yield tetrahydrochalcone (naringenin chalcone). Chalcone isomerase

(CI) then catalyses a stereospecific isomeration of the yellow-coloured tetrahydrochalcone to a colourless flavanone (naringenin). Flavanones act as intermediates for the synthesis of flavones, isoflavones and 3-OH flavanones (dihydroflavonols). Naringenin is converted to dihydrokaempferol (DHK) or to a 3-OH flavanone by flavanone 3-hydroxylase (F3H). The next stage is the conversion of the dihydroxyflavonol to the anthocyanin (Figure 1.4) (Cooper-Driver, 2001).

## **1.10 Anthocyanin synthesis via shikimic acid pathways**

Anthocyanin synthesis is a process that involves many steps from a primary precursor (phenylalanine) to the end products (glycosides of cyanidin) (Figure 1.5) (Wang *et al.*, 2000).

### **1.10.1 Phenylalanine ammonia-lyase (PAL)**

Phenylalanine ammonia-lyase (PAL) is the first enzyme that catalyses the first committed step in the biosynthesis of phenylpropanoids, which performs a variety of functions in plant development and in plant interaction with the environment (Shufflebottom *et al.*, 1993). PAL catalyses the elimination of ammonia (NH<sub>3</sub>) from L-Phenylalanine to give trans-cinnamate (Wang *et al.*, 2000).

Phenylalanine ammonia-lyase activity is affected by many factors, including light, temperature, growth regulators, RNA inhibitors, protein synthesis, tissue damage, pathogen attack, fungicide and herbicide application and the status of certain nutrients (Sanchez *et al.*, 2000).

The localization of phenylpropanoid metabolism in the cytoplasm together with the Shikimate and acetate pathways that supply its precursors have been extensively studied (Winkel-Shirley, 1999). In contrast, Malonyl-CoA is produced by acetyl-CoA carboxylase, which in plants is present in both the cytosol and plastids. The cytoplasmic enzyme is believed to provide malonyl-CoA specifically for chain elongation of C20-C30 fatty acids and the synthesis of flavonoids. However, the subcellular location of the shikimate pathway, the same source of phenylalanine, is still a matter of some debate in plants (Winkel-Shirley, 1999).

#### **1.10.2 Cinnamic acid 4-hydrolase**

Cinnamic acid is converted into coumaric acid by Cinnamic acid 4-hydrolase, which in turn is then modified to the CoA form. Three molecules of malonyl-CoA combine with p-coumaronyl-CoA and form naringerin chalcone, which is then converted into the flavonone, naringenin. This is followed by the formation of dihydroflavonol, which is reduced to flavan-3,4-diol, or leucoanthocyanidin (Holcroft and Kader, 1999).

#### **1.10.3 Anthocyanidin synthase (ANS)**

Anthocyanidin synthase (ANS) converts the colourless leucoanthocyanidins into coloured anthocyanin. ANS is also a 2-oxoglutarate-dependent oxygenase. The reaction involves two steps: In the first step, an active oxoferryl enzyme complex is formed to liberate the succinate and carbon dioxide (CO<sub>2</sub>) by hydrogen radical abstraction and spontaneous dehydration. In the second step, the unstable 2-flavan-3,4-diol intermediate is isomerized spontaneously to 3-flavan-2,3-diol. This compound can immediately be conjugated with UDP-glucose by

flavonoid 3-*O*-glucosyltransferase (3GT) and then transported to the vacuole (Yu *et al.*, 2006).

#### **1.10.4 Flavonoid 3-*O*-glucosyl transferase**

As the final step of anthocyanin core structure biosynthesis, 3GT catalyzes the transfer of glucose from UDP-glucose to the hydroxyl group at C3 of flavonols and anthocyanidins. Anthocyanidins are unstable under physiological pH conditions as they bear a free hydroxyl group, and have to be stabilized by 3GT. The activity of 3GT was first demonstrated in the anthers of maize (Yu *et al.*, 2006). The enzyme is generally cytosolic; the exception being a 3GT from petunia anthers that was primarily associated with membranes. 3GT has been characterized from a number of species using flavonols as substrates and UDP-glucose or UDP-galactose as sugar donor. Glycosylation increases the water solubility of polar flavonoid compounds and improves their stability by external hydrogen bonding of sugar residues with surrounding water molecules. In addition, glycosylation of flavonoids is generally regarded as indispensable for vacuolar transport (Yu *et al.*, 2006).

#### **1.11 Role of bHLH and MYC in anthocyanin synthesis**

Two families of regulators, bHLH (beta helix-loop helix) and MYB proteins, are conserved in the regulation of the anthocyanin and condensed tannins (CT) pathways in all species analyzed to date. The bHLH proteins may have overlapping regulatory targets, while the MYB proteins are the key components providing specificity for subsets of genes activated. For example, AtPAP1 and AtPAP2, which regulate anthocyanin synthesis, and AtTT2, which regulates CT synthesis, are specific for regulation of these branches of flavonoid pathways (Tako *et al.*, 2006).

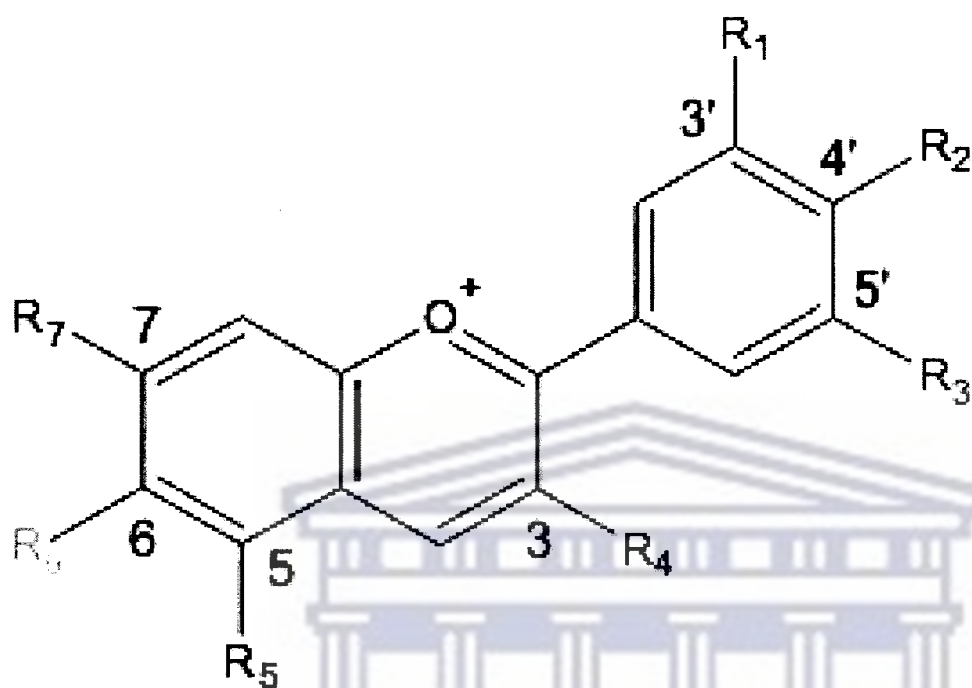


**Figure 1.4:** General structure of anthocyanin (Cooper-Driver, 2001).

UNIVERSITY *of the*  
WESTERN CAPE

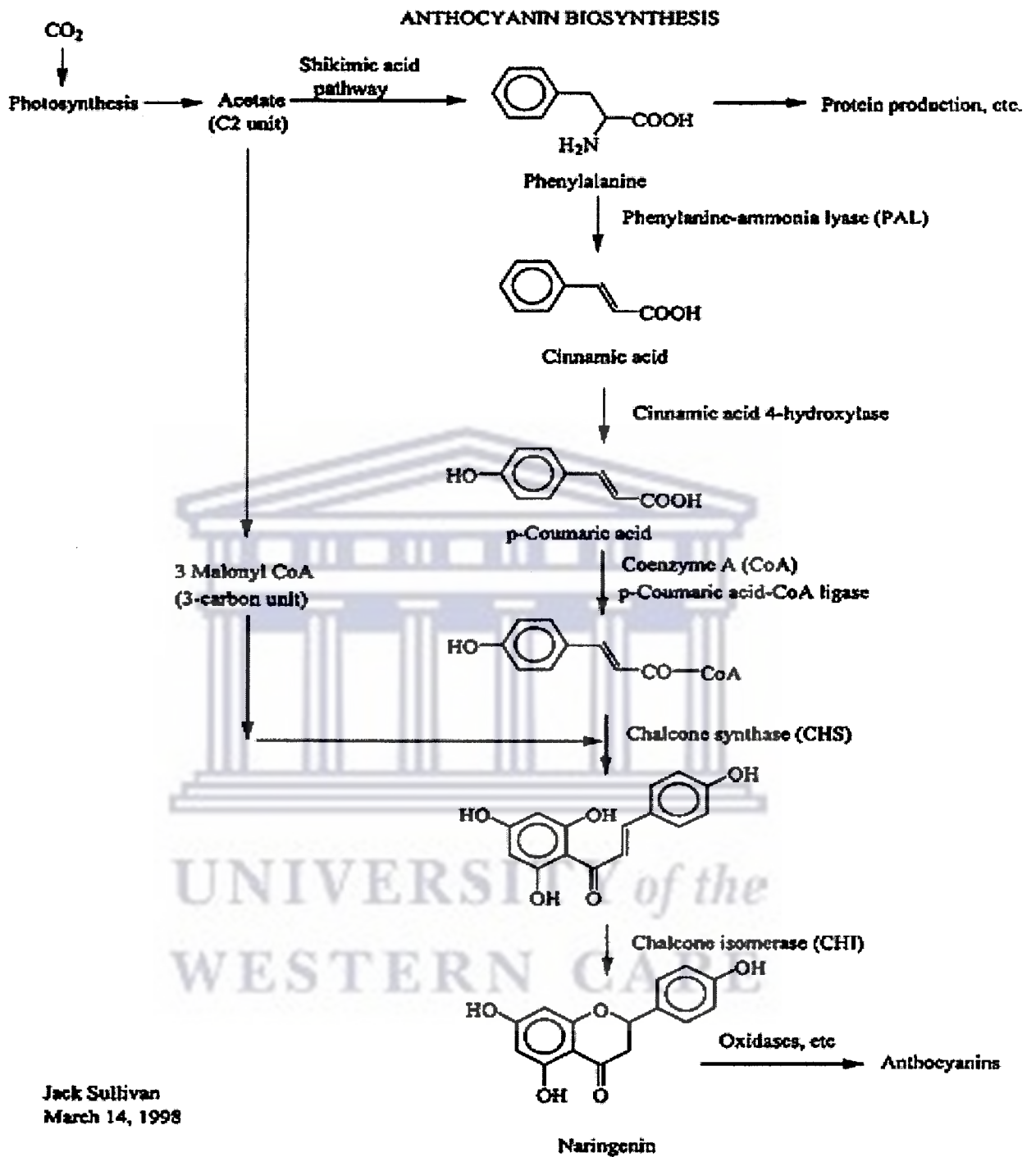


Figure 1.5: General anthocyanin biosynthesis pathway (Sullivan, 1998).

## 1.12 Degradation of anthocyanins

Cytosolic anthocyanin pigments are labile compounds that can undergo a number of degradative reactions (Wrolstad, 2005). Their stability is highly variable depending on their structure and the composition of the matrix in which they exist. Increased glycosidic substitution, and in particular, acylation of sugar residues with cinnamic acids, will increase pigment stability. Polyphenoloxidase, peroxidase, and glycosidase enzymes can have a devastating effect on anthocyanins. These enzymes may be native to the plant tissue, or their source may be from mold contamination. Glycosidase enzyme will act directly on anthocyanins, but the action of polyphenoloxidase and peroxidase is indirect (Wrolstad, 2005). Presence of ascorbic acid will accelerate anthocyanin degradation (Wrolstad, 2005).

## 1.13 Properties of anthocyanin in plants

The most important function of anthocyanins is their ability to impart colour to plants or the plant products in which they occur (Kong *et al.*, 2003). They apparently play a major role in two very different plant processes. Firstly, they attract insects for the purpose of pollination (Sullivan, 1998). Anthocyanin pigments do absorb strongly within the UV (ultraviolet) ranges that are virtually invisible to humans yet at the same time attracting insects. These pigments play a major role in plant pollination and in predation of carnivorous plants where they attract insects into their trap apparatus (Sullivan, 1998). Secondly, anthocyanins must protect plants against strong UV light by absorbing certain wavelengths and in this way prevent DNA damage in the cells. Anthocyanins bind free radicals that usually develop due to plant stress. The above points explain why anthocyanins are located in the epidermal layers of a plant leaves and skin. If plants are exposed to strong UV light or ionising radiation, it in

turn speeds up the process of anthocyanin production over that of other chemical messenger molecules (Chalker-Scott, 1999).

### **1.13.1 Anthocyanins as sunscreens**

Abiotic stress-induced anthocyanin accumulations also predispose leaves to photoinhibition of photosynthesis (Manetas, 2005). For example, under nutrient deficiency the levels of enzymes in the reductive pentose phosphate cycle may decrease. Low temperatures also decrease the activity of these enzymes. As a result, the electron sink capacity of the Calvin cycle is lessened and, in high light, the co-ordination of electron flow and CO<sub>2</sub> assimilation is perturbed (Manetas, 2005). Under these conditions, excitation energy from chlorophyll can lead to oxy-radical production that would result in increased risk of photoinhibitory damage. Leaves somehow afford some sort of an on-line array of biochemical and behavioural means to avoid these risks but in a short-term manner. Firstly, the excess excitation energy can be harmlessly dissipated as heat directly in the pigment bed through activation of the xanthophyll cycle (Manetas, 2005). Secondly, some alternative electron sinks are also available, like the water-water cycle and C<sub>2</sub> photorespiratory cycle which can act as electron valves whenever the sink capacity of the Calvin cycle is surpassed (Manetas, 2005). Furthermore, under prolonged stress, acclimation may still occur through enhancement of the cycles by elevating pool sizes of their components and enzymes while additional biochemical and/or behavioural avoiding reactions may come into play. However, it should be noted that some plants may not display all these extra preventative measures or to some extent, may not display them to appropriate levels. As a result, the severity of stress may finally surpass their acclimative capabilities. Hence anthocyanins act as a sunscreen by attenuating the radiation penetrating the mesophyll and thus reduce the excitation pressure (Manetas, 2005).



### 1.13.2 Anthocyanin as antioxidants

Apart from the direct, light screening function, anthocyanins may indirectly protect plants against excess light through their oxy-radical scavenging properties. They are powerful antioxidants *in vitro* and it may not be irrelevant that the strongest oxy-radical absorbing capacity is displayed by red cyanidin-3-glycoside, i.e. the anthocyanin more often encountered in leaves (Manetas, 2005).

### 1.13.3 Biological activities of anthocyanins

Anthocyanins also possess known pharmacological properties and are used by humans for therapeutic purposes (Kong *et al.*, 2003). Following the recognition that pigment extracts are more effective than *O*-( $\beta$ -hydroxyethyl) rutin in decreasing capillary permeability and fragility, and in their anti-inflammatory and anti-oedema activities it is possible that anthocyanins may replace rutin and its derivatives in the treatment of illnesses involving tissue inflammation or capillary fragility (Kong *et al.*, 2003).

### 1.14 From genomics to proteomics

Following the completion of the genome sequence of *A. thaliana*, many plant scientists have turned the focus on sequencing the genomes of commercially important crops. This initiative by genome researchers will probably contribute towards the understanding of plant biology in general. However, the existence of open reading frames in the genomes does not necessarily relate to the existence of a functional gene, nor can its role in the plant be clearly understood from the genome sequence (Skylas *et al.*, 2004). This increasing number of genome sequences is posing a huge challenge to researchers to identify the functions, modification

and regulation of every encoded protein (Barbier-Brygoo and Joyard, 2004). However, the first stage in annotating any genome is to verify the range of gene products such as polypeptides (its proteome) synthesised in a specific situation (Skylas *et al.*, 2004).

#### **1.14.1 Plant proteomics**

The application of proteomics in plant biotechnology has shown the potential to identify unknown proteins as well as proteins of particular interest. This initiative is fuelled by the rapid availability of plant genome sequences and expressed sequence tags (EST) (Pirondini, *et al.*, 2006). The evaluation of the protein status of cell type tissues, organs and whole organism, is an alternative strategy to address complex biological questions such as the link between the phenotype and genotype (Pirondini, *et al.*, 2006). By definition, proteomics can be referred to as the systematic analysis of a protein population in a tissue, cell, or subcellular compartment (van Wijk, 2001). This technology allows the global analysis of gene products in various tissues and physiological states of cells (Park, 2004). Proteomics aims to supplement analytical techniques designated to study proteins of one species at a time with methodologies that enable thousands of proteins to be studied concomitantly (Hood *et al.*, 2004).

In contrast to the genome, the proteome of a cell is dynamic and changes over time. Proteome analyses are therefore not limited to the description of a current state of protein composition of a cell, but are often used to identify and characterize qualitative or quantitative changes in cellular protein patterns and interactions that can be triggered by external or internal signals (von Neuhoff and Pich, 2005). It is particularly a rich source of biological information because proteins are involved in almost all biological activities and they also have diverse

properties, which collectively contribute greatly to the understanding of biological systems (Patterson and Aebersold, 2003).

While proteomics research is advanced in animals and yeast (Park, 2004), plant proteomics is still in its infancy (Figure 1.6) (Heazlewood and Millar, 2006). Progress in plant proteomics has largely been made by the 2D-based proteomic approaches. Since the resolution of protein spots on 2D gels is limited by factors such as abundance, size and other electrophoretic properties, the complete proteome has been fractionated into sub-proteomes, such as sub-cellular compartments, organelles and multi-protein complexes to improve sensitivity and resolution as well as to reduce overall complexity.

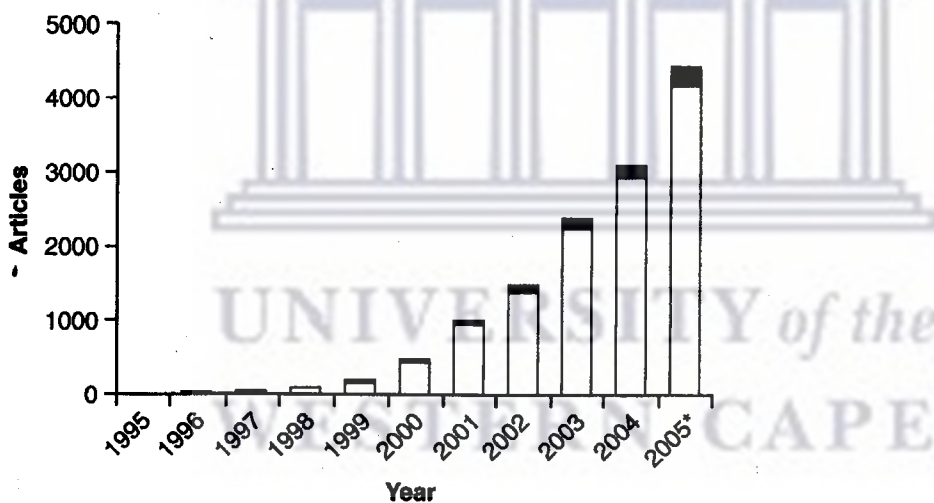


**Figure 1.6:** Number of article using the term proteomics. The searches were conducted using the web from 1995 -2005. The little black box indicates the number of articles that contained the term proteomics (Heazlewood and Millar, 2006).

#### 1.14.2 Where the strength of proteomics lies

The strength of proteomics is based on two key steps which are the separation of proteins by the 2D gels and their subsequent identification by MALDI-TOF. In a standard approach, 2D and mass spectrometry are combined (Xu *et al.*, 2006).

In 2D, the procedure is based on isoelectric focusing (IEF), which separates the proteins based on their isoelectric points (pI), followed by polyacrylamide gel electrophoresis in the presence of sodium dodecyl sulphate (SDS) to separate the proteins on the basis of their molecular weights. The separation parameters allow for the resolution of proteins differing by a single charge, thereby allowing *in vivo* modifications such as phosphorylation and posttranslational modifications to be detected.

During the IEF, the proteins are separated by electrophoresis in a pH gradient. Each type of protein molecule accumulates or focuses, into a sharp spot at its characteristic isoelectric point, defined as the pH at which a protein carries no net electrical charge. Historically, the initial separation for 2D-PAGE by IEF was originally performed in the capillary gels with pH gradient generated by carrier ampholytes. This discouraging task of learning how to handle the fragile capillary gels plus the poor reproducibility of carrier ampholyte IEF led to the wide acceptance of immobilised pH gradient (IPG) for IEF. The pH gradients of IPG are generated by means of buffering compounds that are covalently bound into porous polyacrylamide gels. The pH gradients, fixed as they are in IPG gels, remain stable over extended run times at very high voltages, a requisite for high-resolution separations. IPG are cast on plastic backing sheets and are cut into mechanically stable strips that are easily manipulated (Garfin, 2003).

The high resolving power of 2D-PAGE and the development of various staining procedures to visualize the protein spots have resulted in a very robust methodology for identifying protein abundance and changes between two proteome samples. In conducting such studies, proteome samples from control and treated (or genetically different) cells (or organism or tissue), are extracted and separated on distinct gels. The proteins can be visualized by

colorimetric staining while the spots resolved on both gels are aligned to enable the relative staining intensities of each protein on the gels to be compared. Protein spots that show a difference in staining intensity can be excised from the gel and digested with trypsin and analysed by MALDI-TOF-MS (Hood *et al.*, 2004), (see Figure. 1.7, Bhadauria *et al.*, 2007).

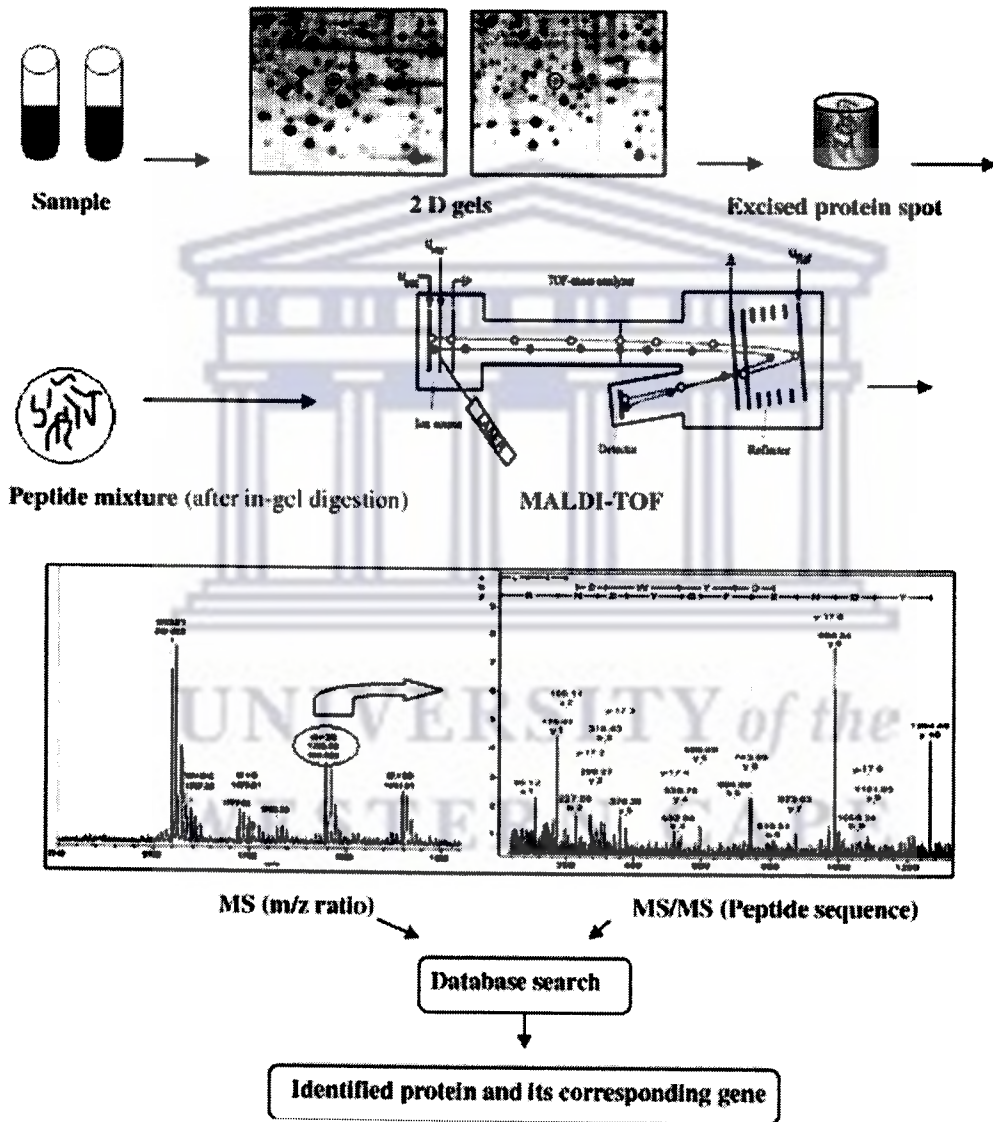


**Figure 1.7:** Overview of common steps involved in protein identification. This procedure typically include sample preparation, separation by 1D SDS-PAGE and 2D-PAGE, followed by protein identification using spectra generated by MALDI-TOF (Bhadauria *et al.*, 2007).

## **1.15 Gel visualization**

Following gel electrophoresis, the next steps are protein staining and image analysis in order to quantify each protein and to allow qualitative comparison of samples (Rose *et al.*, 2004). Despite the availability of a wide range of specific stains, the majority of 2D-PAGE gels are stained with Coomassie brilliant blue (CBB) and SYPRO Ruby (Garfin, 2003).

### **1.15.1 Coomassie brilliant blue (CBB)**

CBB is an anionic triphenylmethane dye which binds to proteins non-covalently. This post-electrophoretic stain requires an acid medium for the electrostatic interaction between the dye molecules and the amino groups of the proteins. After the fixation of the proteins, the gel becomes saturated with the dye solution which can be destained later. The detection limit of this stain solution is reported to be less than 100ng of protein (Gorg and Weiss, 2004).

### **1.15.2 SYPRO Ruby**

SYPRO Ruby is a fluorescent dye which detects protein by binding to them non-covalently. This staining solution may bind directly to the proteins or to the detergent coating the protein. The proteins are stained by simply soaking the gel in the solution containing a fluorophore. This solution does not change the nature of proteins or interfere with post-electrophoretic analysis of proteins such as mass spectrometry (Gorg and Weiss, 2004).

## **1.16 Principles and instrumentation of Mass spectrometry**

Briefly, mass spectrometric measurements are carried out in the gas phase on ionised analytes. By definition, a mass spectrometer consists of an ion source, a mass analyser that measures the mass to charge ratio ( $m/z$ ) of the ionised analytes and detector that registers the number of ions at each  $m/z$  value. Electrospray ionization (ESI) and Matrix-assisted laser

desorption/ionisation-time-of-flight (MALDI-TOF) are the two techniques most commonly used to volatize and ionize the proteins or peptides for mass spectrometric analysis (Aebersold and Matthias, 2003).



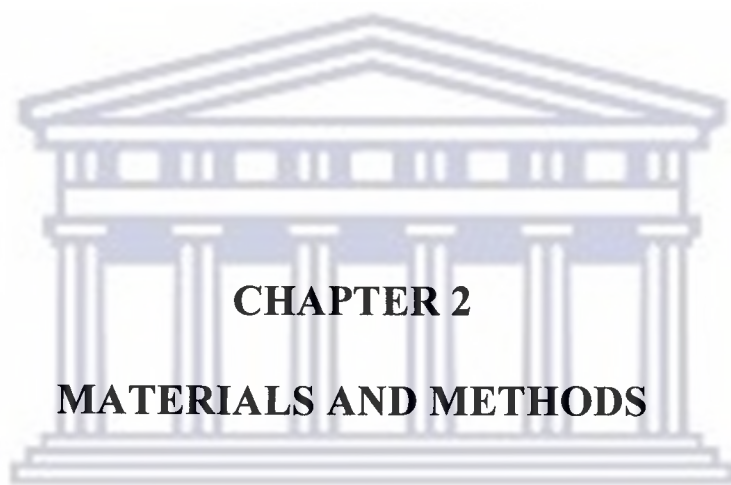
### 1.17 Objectives

The principal objective of this study was to investigate the molecular determinants of red and green colouration in pear tissues using proteomics techniques. I intended to achieve this goal using the following experimental approaches:-

- i. To generate and construct 2D proteome profiles of various pear fruit crop tissues (leaf, skin and pulp),
- ii. To produce an initial 2D proteome profile maps of these selected tissues
- iii. To visualise, quantify and identify differentially expressed proteins between the 'Bon Rouge' pears (red versus green)







**CHAPTER 2**

**MATERIALS AND METHODS**

UNIVERSITY *of the*  
WESTERN CAPE

## 2.1 Materials

### 2.1.1 The pear leaf materials

The 'Bon Rouge' pear leaf material was obtained from Agricultural Research Council (ARC) experimental farm located in the Western Cape province of South Africa. The leaves were collected periodically on the 06 October 2006, 01 November 2006, 12 December 2006 and 07 March 2007. The leaves were split into two major groups of seedlings and clones respectively as shown in Table 2.1 below.

The 'Bon Rouge' pear cultivar was developed from a bud mutation that has been reported to occur only once on a Williams 'Bon Chretien' (Bartlett) pear cultivar. The bud spot was discovered on a 'Bon Chretien' tree by D. Mouton on his farm Ongegund, Simondium (Western Cape province, South Africa) and 'Bon Rouge' was released by the Stellenbosch Institute for Fruit Technology (INFRUITEC), South Africa in 1993 (Jolly, 1993). Branches from 'Bon Rouge' and reverted 'Bon Rouge' branches were cloned onto rootstock and planted in an orchard on the experimental farm at Bien Donne. Clones were labelled according to the tree number in the original commercial orchard from which they were derived.

**Table 2.1:** Plant leaf material from pear trees

Seedlings	Clones
'Bon Rouge'	BR1; BRR1
'Bon Rouge' Revertant	BR7; BRR7
	BR8; BRR8
	BR9; BRR9
	BR16; BRR16
	BR22; BRR22

### 2.1.2 Pear fruits material

Pear fruit skins (red and green) and pulps from 'Bon Rouge' and 'Bon Rouge' revertant were used for extracting protein, protein quantitation, 1D SDS-PAGE and 2D-PAGE.

### 2.1.3 Sampling, delivery and storage of pear material

During the sampling, pear leaves were kept and transported in liquid nitrogen from the farm. They were then stored at  $-80^{\circ}\text{C}$  until the day of protein extraction. Pear fruits on the other hand were transported from the farm to the laboratory at room temperature. In the laboratory, the fruits were peeled using a vegetable peeler to separate the skin from the pulp. Both the skins and pulps were stored separately at  $-80^{\circ}\text{C}$  freezer in the laboratory until the day of protein extraction.

### 2.1.4 Chemicals

Table 2.2 below shows the names of all the chemicals used during the period of study, the names of the companies they were purchased from and as well as the catalogue numbers. The chemicals were listed according to their alphabetical order.

**Table 2.2: List of chemicals**

Chemicals	Company	Catalogue no.
Acetone	Merck	102 20 40 LC
Acetonitrile	Merck	1. 00030. 2500
Agarose	Whitehead Scientific	D-1 LE
Ammonium bicarbonate	Promega	1.011 31. 5000
Ammonium Persulphate (APS)	Sigma	A3678-100G
Ampholytes	BIO-RAD	163-2094

40 % (37.5:1) Acrylamide: bis-acrylamide	BIO-RAD	161-0148
Bovine Serum Albumin (BSA)	ROCHE	10 735 078 001
Bradford assay solution	BIO-RAD	500-0006
Bromophenol Blue	Sigma	B5525-10G
Coomassie Brilliant Blue R-250	BIO-RAD	161-0400
CHAPS (3-[(3-Cholamidopropyl) dimethylammonio]-1-propanesulfonate)	Sigma	C3023-5G
Dithiothreitol (DTT)	Fermentas	R0861
Ethanol 99.7-100%	Kimix	33/0807
Glacial acetic acid	Merck	102 10 00 LC
Glycerol	Sigma	G5516-1L
Glycine	Sigma	G-7126
Hydrochloric acid	Merck	306 30 40 LP
Iodocetamide	BIO-RAD	163-2109
Mineral oil	GE Healthcare	17-1 335-01
PageBlue™ Protein staining solution	Fermentas	SM0661
Propan-2-ol (Iso-propyl alcohol)	Merck	507 50 40 LC
Sodium dodecyl sulfate (SDS)	BIO-RAD	161-0302
TEMED (N, N, N <sup>1</sup> ,N <sup>1</sup> - tetra methylethelene-diamine)	BIO-RAD	161-0801
Thiourea	Sigma	T8656-100G
Trichloroacetic acid (TCA)	Merck	6110500 EM
Trifluoroacetic acid	Merck	8. 08260. 0100
Tris (hydroxymethyl) aminomethane	BIO-RAD	161-0719
Trypsin	Promega	V5111

### 2.1.5 General stock solutions and buffers used during the period of study

10x SDS-PAGE buffer	1% SDS (w/v), 3.03% Tris (w/v) and 14.41% glycine (w/v) in distilled water.
10% SDS solution	10% SDS (w/v) in distilled water.
1x SDS-PAGE buffer	10% SDS-PAGE buffer (v/v) in distilled water
APS solution	10% Ammonium persulphate (w/v) in distilled water.
50 mM ammonium bicarbonate	50 mM Ammonium bicarbonate (w/v) in distilled water.
Stacking SDS-PAGE	5% Arcylamide solution (37. 5:1) (v/v), 0.125 M Tris, 0.05% SDS (v/v), 0.05% APS (v/v), 0.006% TEMED (v/v).
Resolving SDS-PAGE	12% Arcylamide solution (37. 5:1) (v/v), 0.375 M Tris, 0.1% SDS (v/v), 0.1% APS (v/v), 0.004% TEMED (v/v).
2x SDS-PAGE sample buffer	0.15 M TRIS (pH 6.8), 1.2% SDS (w/v), 0.3% glycerol (v/v), 0.15% $\beta$ -mercaptoethanol (v/v), 0.0018% bromophenol blue (w/v).
SDS-PAGE Equilibration buffer I	6 M Urea, 0.375 M Tris-HCl, pH 8.8, 2% SDS (w/v), 20% glycerol (v/v), 1% DTT (w/v).
SDS-PAGE Equilibration buffer II	6 M Urea, 0.375 M Tris-HCl, pH 8.8, 2% SDS, 20% glycerol, 2.5% (w/v) iodoacetamide.

70% Ethanol	70% absolute ethanol (99.5%) (v/v) in distilled water.
CBB staining solution I	10% glacial acetic acid, 2% CBB stock solution, 25% propan-2-ol.
CBB staining solution II	10% glacial acetic acid (v/v), 0.25% CBB Stock solution (v/v), 10% propan-2-ol.
CBB staining solution III	10% glacial acetic acid (v/v), 0.25% CBB stock solution (v/v).
CBB destaining solution	10% glacial acetic acid (v/v), 1% glycerol (v/v) in water.
50% Acetonitrile	50% acetonitrile (v/v) in distilled water.
50% DTT	50% DTT (w/v) in protein extraction buffer.
10% TCA	10% TCA (w/v) in water.
80% Acetone	80% absolute acetone (v/v) in water.
1% TFA	1% TFA acid (v/v) in distilled water.
Protein extraction buffer	9 M urea, 2 M thiourea and 4% CHAPS.
CBB stock solution	1.25% Coomassie brilliant blue (w/v) in distilled water.
Trypsin	10 µg/ ml Trypsin (w/v) in ammonium bicarbonate buffer.

## **2.2 Methods**

### **2.2.1 Protein extraction**

#### **2.2.1.1 Protein extraction from pear leaves**

Total soluble proteins (TSP) were extracted from mature pear leaves. Approximately 1 g of pear leaves was ground to a fine powder in liquid nitrogen and 1ml of 10% TCA was added to the ground material with the brief continuation of grinding of about thirty seconds. The ground material was placed in 1.5 and/or 2 ml tubes. The tubes were then spun in the centrifuge at 13 200 x g for 10 minutes in the cold room and the TCA supernatant was removed. The pellets were washed 2-3 times with 80% ice-cold acetone (to ensure that the pellet was fully dispersed and all the residual amounts of TCA were removed). The tubes were left to dry at room temperature for about 5-10 minutes, until no visible amount of acetone was left on the side of the tube. The pellets were re-suspended in approximately 300 µl of the extraction buffer and the homogenate was incubated on ice for about 30 minutes. The homogenate was vortexed in the cold room overnight. On the following day, the homogenate was centrifuged in the cold room for about 10 minutes at 13 200 x g and the supernatant, which contained the whole cell protein (TSP), was thereafter transferred to a new sterilised 1.5 and/or 2 ml tubes. Protein quantification was performed using a modified Bradford assay (Bradford, 1976), as described by Ndimba *et al.*, (2003) and about 20 µg of protein was electrophoresed on a 12% SDS-PAGE at 120 V for ninety minutes.

#### **2.2.1.2 Protein extraction from pear fruits**

Protein extraction from pear fruit skin and pulp was carried out in the same way as pear leaf material (as in section 2.4.1) except that the pellets were re-suspended in ReadyPrep™ Protein Extraction Kit (BIO-RAD, Hercules, CA, USA) prepared according to the

manufacturer's instruction. The samples were electrophoresed on 12% SDS-PAGE at 120 V for ninety minutes.

### **2.2.2 Protein Quantification**

Protein concentration on the extracts was estimated using the modified Bradford assay method (Bradford, 1976), as described by Ndimba *et al.*, (2003), using Bovine serum albumin (BSA) as a standard to generate the calibration curve. The BSA standard solution of 5 mg/ml was prepared and aliquot into different concentrations and this was adjusted to the total volume of 10  $\mu$ l different volumes of extraction buffer before other components were added as shown in Table 2.2. The protein quantification of tissues of interest from pear materials was also prepared at the same time when the BSA standard solutions were prepared as shown in Table 2.3, i.e. total soluble protein (5  $\mu$ l) from tissues of interest was adjusted to the total volume of 10  $\mu$ l with extraction buffer before other components were added. After all the components were added into cuvettes, the absorbance was measured at a wavelength of 595 nm using the Genesis 5 Spectrophotometer (Milton Roy, Groton, CT, USA).

UNIVERSITY *of the*  
WESTERN CAPE



**Table 2.3:** Preparation of BSA standard solutions for Bradford Assay for generation of a standard curve.

Final concentration ( $\mu\text{g}/\mu\text{l}$ )	Volume of BSA standard stock solution (5mg/ml) ( $\mu\text{l}$ )	Volume of extraction buffer ( $\mu\text{l}$ )	0.1M HCl ( $\mu\text{l}$ )	dH <sub>2</sub> O ( $\mu\text{l}$ )	Bradford solution ( $\mu\text{l}$ )
0	0	10	10	80	900
5	1	9	10	80	900
10	2	8	10	80	900
20	4	6	10	80	900
40	8	2	10	80	900
50	10	0	10	80	900

**Table: 2.4** Protein quantification of pear plant tissues

<b>Sample</b>	5 $\mu\text{l}$
<b>0.1M HCl</b>	10 $\mu\text{l}$
<b>Distilled water</b>	80 $\mu\text{l}$
<b>Extraction buffer</b>	5 $\mu\text{l}$
<b>Bradford reagent</b>	900 $\mu\text{l}$

### **2.2.3 1D SDS-PAGE**

Protein samples were separated on 1D SDS-PAGE according to Laemmli's method (Laemmli, 1970). This protocol utilises the preparation stacking gels to load the protein samples and resolving gels for protein separation. The gels of 1mm thicknesses were cast using gel plates with permanent bonded gel spacers (BIO-RAD) using a Mini-PROTEAN<sup>R</sup> 3 Cell gel casting system (BIO-RAD). The 12% resolving gel was cast first and overlaid with 200 µl of isopropanol before the gel was left to polymerize at room temperature. The gap of about 1.5 cm between the top of the glass plates and the 12% resolving gel was left in order to allow the 5% stacking gels to be added. Prior to the addition of 5% stacking gels the isopropanol overlay was decanted and the gels were rinsed with distilled water. Immediately upon casting the 5% stacking gel the 10 well combs was inserted. The 5% stacking gel was allowed to polymerize for few minutes and the combs were removed from the gels and the gels were ready for use. Protein samples were prepared by mixing 20 µg of protein sample with equal volume of 2x SDS-PAGE sample buffer. The samples were vortexed briefly and boiled at 95°C for 5 minutes. Electrophoresis was carried out in 1x SDS-PAGE running buffer using a Mini-PROTEAN<sup>R</sup> 3 Cell (BIO-RAD) for 90 minutes. The gels were stained in Coomassie brilliant blue staining solution as described in Section 2.2.4.

### **2.2.4 Staining of the gels**

After electrophoresis, the gels were gently removed from the glass plates and stained in Coomassie brilliant blue solution I, II, and III respectively for about 30 minutes in each solution. Prior to each staining step, the gels were immersed into the staining solution and heated in a microwave for about 1 minute. Staining was done with shaking on an orbital shaker for 30 minutes in each stain. Once the staining steps were completed, the gels were destained up until the desired bands/spots intensity was achieved.

## **2.2.5 Second dimensional gel electrophoresis preparation**

### **2.2.5.1 Reswelling of IPG strips**

Immobiline pH gradient (IPG) Strips (7 cm; pH 4-7, BIO-RAD), were rehydrated overnight at room temperature in a total volume of 125  $\mu$ l of rehydration buffer containing (2  $\mu$ l of 50% DTT, 1.25  $\mu$ l of ampholytes (pH 3-10), 150  $\mu$ g of protein sample, and this was adjusted with urea lysis buffer to constitute a total volume 125  $\mu$ l) in a rehydration tray. The cover foil was carefully removed from the IPG strip without damaging the gel and the IPG strip was gently placed in the tray channel gel side facing down, avoiding to trap air bubbles under the strip. The IPG strip was overlaid with mineral oil and allowed to rehydrate overnight at room temperature.

### **2.2.5.2 Isoelectric focusing (IEF) of the IPG strips**

After overnight rehydration, the IPG strips were removed from the rehydration tray and rinsed with distilled water and loaded on an IEF machine (Ettan<sup>TM</sup>IPGphorII<sup>TM</sup> IEF machine, GE Healthcare, Amersham, UK) with the gel side facing upward. The IPG strips were overlaid with mineral oil and the IEF machine was programmed to three stepped phases running protocol [Step 1: 200 V for 0:10h; Step 2: 3500 V for 2 800 Vhr; Step 3: 3 500 V for 3 700 Vhr].

After IEF, the IPG strips were removed and rinsed with distilled water and blotted on a wet filter paper. The IPG strips were placed back in the clean rehydration tray and incubated in equilibration buffer I containing DTT for about 10 minutes with gentle shaking at room temperature. At the end of the 10 minutes incubation, SDS-PAGE equilibration buffer I was decanted from the tray. The IPG strips were further incubated in the SDS-PAGE equilibration buffer II, which contained iodoacetamide for 10 minutes with gentle shaking at room

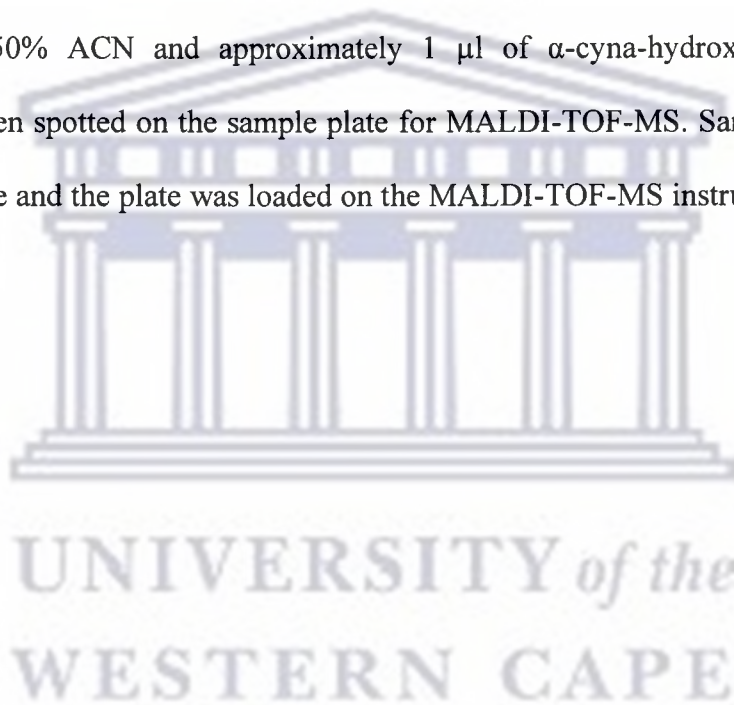
temperature. After the second equilibration step the IPG strips were removed and rinsed with 1X SDS-PAGE running buffer. The IPG strips were then placed on top of 12% gels, with the gel side of the IPG strip facing towards the smaller plate. The IPG strips were finally overlaid with 0.5% agarose sealing solution, which was allowed to solidify for 5 minutes before the gels were mounted in the electrophoresis cell. The gels were run at 120 V for about ninety minutes.

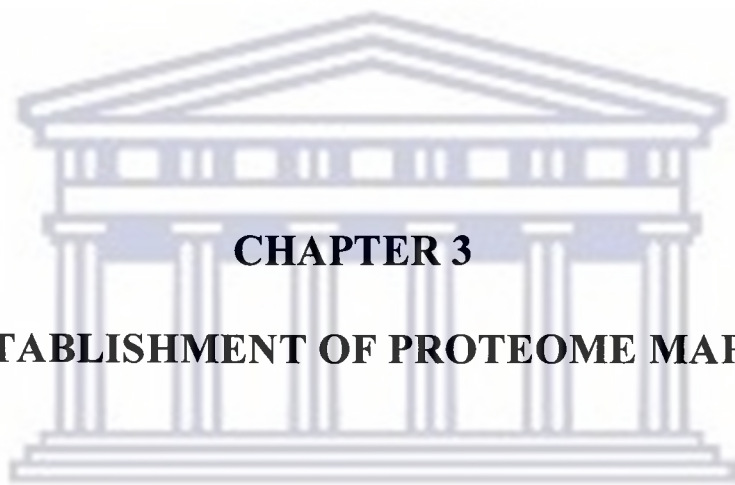
### **2.2.6 In-gel digestion of protein spots from the 2D gels**

Spots differing in intensity between the two comparative 2D gels were excised. The gel pieces were transferred into separate eppendorf tubes that were filled with 50 mM ammonium bicarbonate buffer. This washing step was performed two times with five minutes incubation and in each wash step the solution was discarded at the end. After the washing step, 500  $\mu$ l of 50 mM ammonium bicarbonate buffer were added and the samples were incubated for 30 minutes with occasional vortexing. After 30 minutes of incubation ammonium bicarbonate buffer was discarded.

The gel pieces were then washed two times using 100  $\mu$ l of 50% ammonium bicarbonate buffer and 50% (v/v) acetonitrile for 30 minutes with occasional vortexing. This step was repeated two times for complete destaining of gel pieces. 100  $\mu$ l of 100% acetonitrile was then added enough to completely cover the gel pieces in case of many pieces of the same sample. Samples were incubated on the bench top for 5 minutes, to allow gel pieces to turn whitish. The gel pieces were then completely dried using a speed vacuum drier (Speed Vac SC100 (Savant), LASEC, Old Moll Road, Cape Town, RSA). About 10  $\mu$ l of trypsin (10  $\mu$ g/ml) was added to the dried gel pieces and incubated at 37°C for overnight.

After incubation the digestion process was stopped by the addition of 50-100  $\mu$ l of 1% TFA and left for 2-4 hours at room temperature before samples were stored at 4°C until further analysis. Micro C<sub>18</sub> zip tips were used to clean-up the sample for loading on the sample plate for identification on the Matrix assisted laser desorption ionisation time of flight (MALDI-TOF-MS) instrument (Voyager-DE™ PRO Biospectrometry™ workstation, Applied Biosciences, Forster City, CA, USA). Zip tips were first configured in three solutions; 100% ACN, 50% ACN and milliQ water respectively. After this step the peptides from the protein to be identified was bound to the column (zip tip) and then eluted on to the MALDI-TOF-MS plate wells with 50% ACN and approximately 1  $\mu$ l of  $\alpha$ -cyna-hydroxy-cinnamic acid (CHCA) matrix, then spotted on the sample plate for MALDI-TOF-MS. Samples were dried at room temperature and the plate was loaded on the MALDI-TOF-MS instrument for protein identification.





**CHAPTER 3**

**ESTABLISHMENT OF PROTEOME MAPS**

UNIVERSITY *of the*  
WESTERN CAPE

### **3.1 Introduction**

Proteomics is a tool that can be used to study protein-related molecular events underlying plant growth, development and their responses to environmental cues (Di Michele *et al.*, 2006). Hence, the objective of this chapter was to generate 2D proteome reference maps of pear fruit crops using proteomic approaches. Currently, there is no study done or reported on the generation of 2D reference maps of pears.

To date, proteomics research relies on the application of the two-dimensional polyacrylamide gel electrophoresis (2D-PAGE) to generate the proteome reference maps under various growth conditions. Thus far, 2D-PAGE is the only higher resolution gel based method for large-scale quantitative comparison of changes in protein profiles of cells, tissues, or whole organisms (Zuo and Speicher, 2000).

In this study, pear plant material was sub-divided into three categories i.e. leaves, fruit skins and pulps. Several fruit skins from several pear fruits were combined together to form one extract in order to increase the protein concentration and to reduce the running expenses. The same approach was applied to fruit and pulps.

### **3.2 Results and discussion**

#### **3.2.1 Optimization of protein extraction and 1D SDS-PAGE**

This section describes the optimisation of protein preparation protocols. The pear materials was ground and precipitated in the presence of TCA and liquid nitrogen. The pellets were washed to remove the materials that interfere with gel resolution such as organic acids, phenolic compounds, pigments and inhibitory ions. The total soluble proteins were extracted from tissues of interest (leaves, pulps and fruit skins) by using urea/thiourea lysis buffer. Urea

serves as a chaotropic substance and its role, in the solubilisation process, is to break the non-covalent interactions between the various molecules present in the sample such as hydrogen bonds, dipole-dipole interactions, and hydrophobic interaction, and to unfold the proteins. The presence of thiourea, as an additional chaotrope, also helps towards the improvement of solubilisation of proteins and limits protease activities.

This extraction protocol produced the highest quality of protein extracts and managed to recover most of the lower molecular weight proteins which usually escape in many protein extraction protocols that are not optimised for protein extraction from plants tissues. The concentration of proteins samples was quantified using modified Bradford Assay (Bradford, 1976) as in Section 2.2.2. Concentrations of protein extracted from pulp, fruit skin and leaf of the pear are shown in Table 3.1. Protein concentration for all three tissues samples fluctuated. However, on average protein concentration for leaf was 0.8  $\mu\text{g}/\mu\text{l}$  before optimization and improved to 7.6  $\mu\text{g}/\mu\text{l}$  after optimization for pulp 0.3  $\mu\text{g}/\mu\text{l}$  before optimization and improved to 3.6  $\mu\text{g}/\mu\text{l}$  after optimization and for the fruit skin 0.2  $\mu\text{g}/\mu\text{l}$  before optimization and improved 2.8  $\mu\text{g}/\mu\text{l}$  after optimization as shown in Table 3.1. The quality of the total soluble proteins extracted from the tissues was determined on 1D SDS-PAGE as in Figure 3.1A and B. This figure shows the quality of protein extracts from the 'Bon Rouge' pear tissues. Further on, protein samples evaluated on the 1D SDS-PAGE were used in the establishment of the 2D-PAGE proteome maps of pear fruit crop.

As already mentioned, Figure 3.1A and B shows the success of protein extraction optimisation and mostly the establishment of proteome profile for 'Bon Rouge' pears. In Figure 3.1A lane 1 shows molecular weight markers, lane 2 shows pulp protein extract and



lane 3 was fruit skin extract, respectively. Figure 3.1B lane 1 show molecular weight markers and lane 2 was the leaf extract of the pear fruit.

From Figure 3.1A and B it is clear that protein molecular weights from all tissues ranged from 120 kDa to 15 kDa most proteins ranging between 200 kDa and 10 kDa. Some of the proteins were most abundant as they appear darker upon Coomassie staining in all tissue samples. Coomassie brilliant blue is a semi quantitative protein stain and binding intensity is proportional to the abundance of the protein represented by the band. The most abundant protein were in the following molecular weight ranges; at about 100 kDa, between 85 and 70 between 60 and 50 kDa and lastly between 45 and 30 kDa. The most abundant protein was found at 53kDa.

Mapping of the gel depicted in Figure 3.1 thus proved to be interesting as each induced protein has a specific function in cell biology. It must be noted that the protein profile in Figure 3.1B appears to be slightly different because the 1D SDS-PAGE was experiment was performed on a separate day, but there is consistency in protein induction at the same regions as already mentioned. Figure 3.1C shows the protein extracts before the optimisation with faint bands and this protocol used was not used in any of the subsequent experiments.

**Table 3.1:** Shows average protein concentration from pear tissue

Sample	Average concentration before optimisation ( $\mu\text{g}/\mu\text{l}$ )	Average concentration After optimisation ( $\mu\text{g}/\mu\text{l}$ )
Leaf	0.5	7.6
Pulp	0.3	3.6
Fruit skin	0.2	2.8

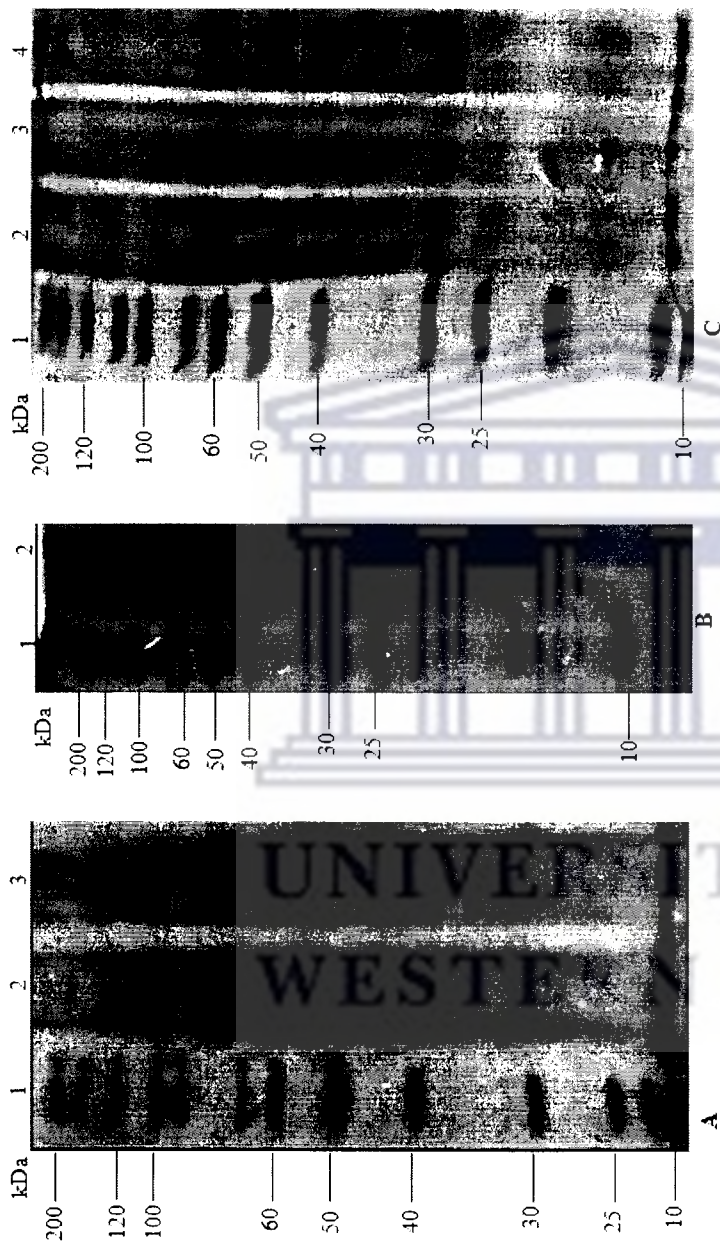


**Figure 3.1** 1D SDS-PAGE profiles of TSP from pear tissue (A) Lane 1 shows molecular weight marker, lanes 2 and 3 show pulp and fruit skin proteins respectively. (B) Lane 1 shows molecular weight marker and lane 2 shows pear leaf proteins. (C) Shows protein extracts before optimisation. Lane 1 shows molecular weight marker, lanes 2-4 show pulp, fruit skin and leaf respectively. Approximately 20  $\mu\text{g}$  of pear fruit crop tissues protein samples were separated on 12% SDS polyacrylamide gels. The gels were stained with Coomassie brilliant blue R-250 and images captured by Phoros FX<sup>TM</sup> plus molecular imager scanner (BIO-RAD).

### **3.2.2 Establishment of 2D-PAGE proteome maps of Pear tissues**

Before the 2D proteome map could be established, a number of parameters such as pH range of the IPG strips and the duration of IEF step needed to be optimised. During the IEF step temperature and current remained constant whereas the duration of focusing the IPG strips was scaled down from a total of 10 000 v/h to a total of approximately 7 500 v/h. Various pH ranges for IPG strips were also used, starting with the wider pH scale (pH 3-10) and scaling it down accordingly until the maximum spot resolution was obtained. Figure 3.2A and 3.2B show the various effects associated with pH range of the strips and focusing period respectively. It was finally established that duration of the IEF step is dependent on both the sample conductivity and protein loading.

It was further observed that IEF step produced good spots resolution if performed to a total of approximate value of 7 500 v/h on the 7 cm strip of pH range 4-7. Figure 3.3A-C shows the well resolved protein spots on the 2D proteome maps. The optimization of IEF running parameters in this study demonstrated that they are of significant importance as the IPG strips may sometimes be under or even over focused at some stage as it was seen in Figure 3.2B. Both these factors will certainly lead to a poor resolution of protein spots. Apart from general problems associated with protein work, other problems are frequently encountered in many biological samples during the IEF.

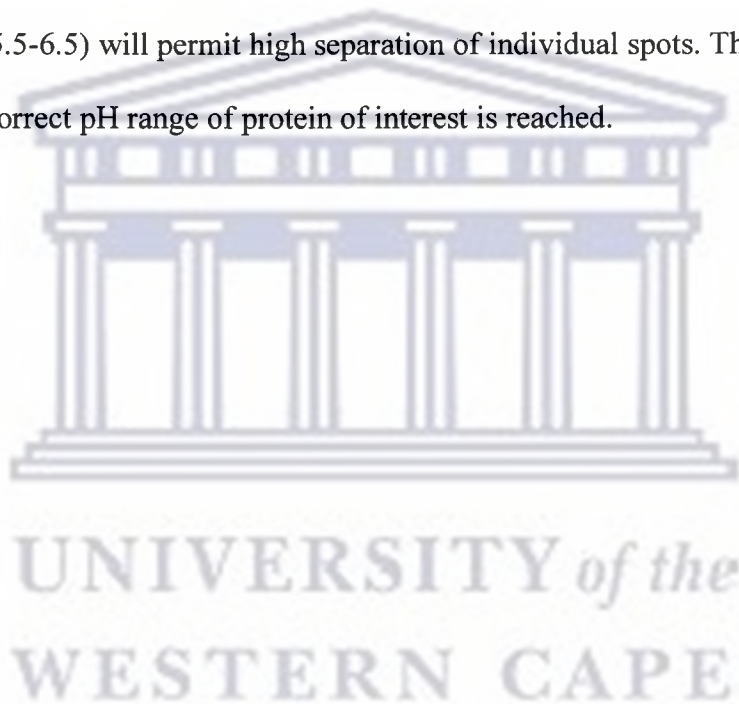
These problems arise from non-protein compounds that can be present in the sample. For example, nucleic acids can completely blur the 2D gel pattern when present at too high a concentration. Nucleic acids act as mobile ion exchangers at the low ionic strength required by IEF, thereby creating severe artefacts. Other classes of compounds (lipids, salts etc.) can be encountered in many samples and create their artefacts. This is especially true for the

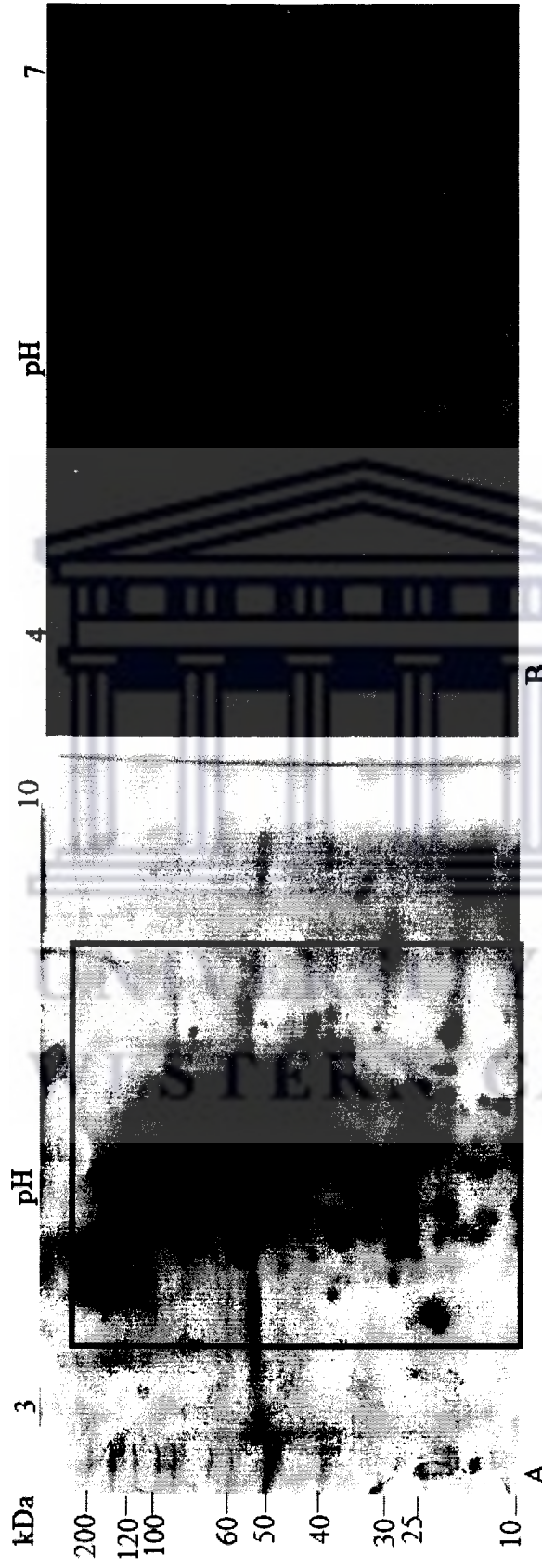
plant-derived samples, due to the ability of plant tissues to synthesize a host of compounds with varied structures (Heazlewood and Millar, 2006). For example, phenolics and chlorophyll can be very abundant in some plant tissues and completely ruin protein separation in proteomics.

Figure 3.3 shows successful establishment of protein profiles from pulp, leaf and fruit skin, respectively. Proteins on these 2D gels were separated over a wide range of molecular weights ranging from 200 kDa to 10 kDa for all tissues. More abundant proteins were found mostly in the region of 200 kDa and 30 kDa and a few below 30 kDa for the pulp tissue. 2D gels of leaf tissue extract (Figure 3.3B) shows the most abundant proteins to be in the region of 100 kDa and below 15 kDa. The skin tissue extract had the least number of proteins (Figure 3.3C), with the most abundant proteins in the region between 60 kDa and 50 kDa. The less-abundant proteins on the skin of the fruit (Figure 3.3C) mostly appeared in a straight line suggesting that it could be the same protein but modified for a specific function.

In total the number of proteins spot is less abundant in Figure 3.3C. Normally a skin's biological function is to serve as a barrier between the soft tissues and the environment. At this stage 2D-PAGE showed a small number of proteins on the skin. When comparing 1D SDS-PAGE (Figure 3.1) gels and 2D-PAGE gels (Figure 3.3), on 1D SDS-PAGE it appears as if there is equal levels of protein abundance in all tissues i.e. skin, pulp and leaves of pear while in 2D there is overwhelming difference on levels of protein abundance in all tissues. This emphasises the importance of 2D PAGE in protein profiling as protein are separated according to *pI* and molecular weight.

However, all the tissues analysed in this study were found to have better spot resolution at pH ranges between 4 and 7 as seen Figure 3.3, though various pH ranges were tested during the preliminary test, trying to locate the pH ranges that will give best resolution of protein spots from tissues of interest. During the broad range (pH 3-10) analysis, the proteins spots were observed to be clustered towards the centre of the gel (Figure 3.2A), indicating that a narrow pH range was required for increased resolution. However, it is important to start with a broad range (pH 3-10), as this will show the whole spectrum of proteins components expressed in a whole cell, tissue and organ and scaling it down to the mid-range (pH 4-7, 5-8, and 6-11) and narrow range (pH 5.5-6.5) will permit high separation of individual spots. This step should be repeated until the correct pH range of protein of interest is reached.





**Figure 3.2** 2D profiles showing poor gel resolution (A) Gel run on a large scale pH range (3-10, BIO-RAD) with protein spots clustering towards the centre of a gel, highlighted area shows the clustered spots on the centre of a gel. (B) Gel run on a mid-scale pH (4-7, BIO-RAD) showing the effects of less or over focusing of the IPG strips, highlighted area show the affected area with horizontal streaks. Approximately 150  $\mu\text{g}$  of pear tissues (leaf and fruit skin) protein samples were isoelectric-focused on a 7 cm IPG strips (pH 3-10 and 4-7 respectively) and then separated in the second dimension on a 12 % SDS polyacrylamide gels. The gels were stained with Coomassie brilliant blue R-250 and images captured by Pharos FX<sup>TM</sup> plus molecular imager scanner (BIO-RAD).

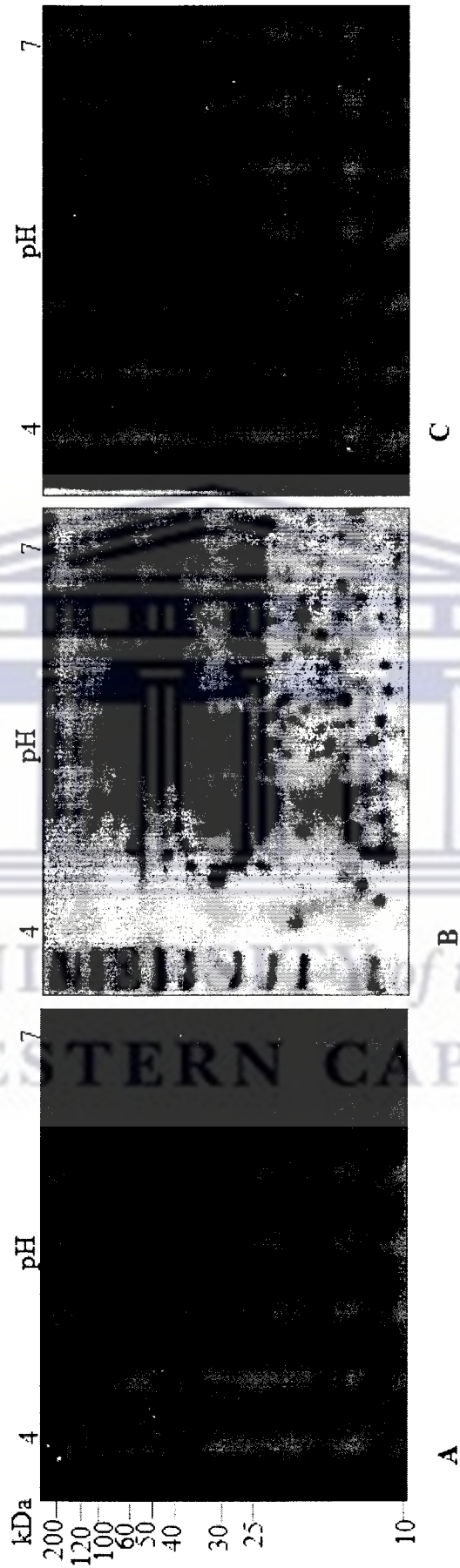
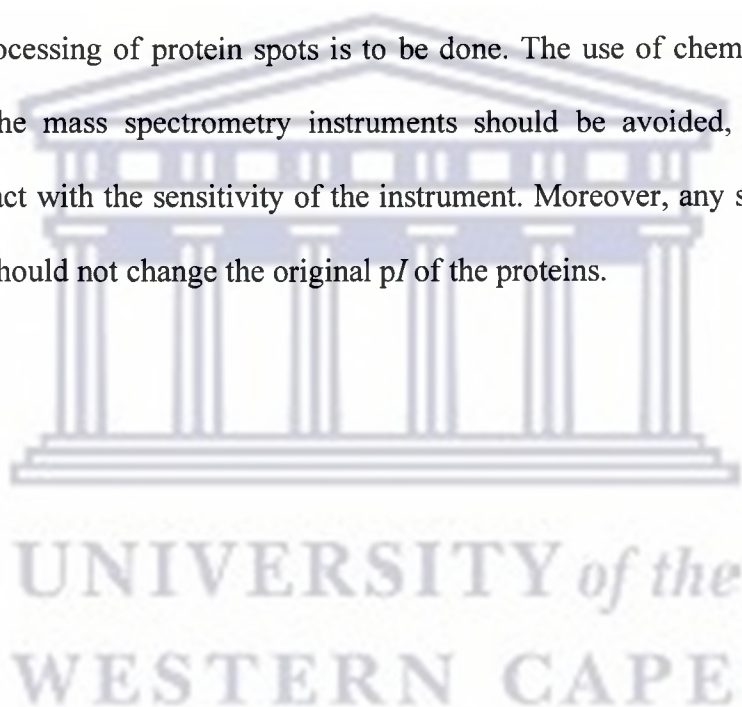


**Figure 3.3** Established proteome maps of total soluble proteins from pear tissue. Approximately 150  $\mu\text{g}$  of pear tissues protein samples were isoelectric-focused on a 7 cm IPG strips (pH 4-7, BIO-RAD) and then separated in the second dimension on a 12 % SDS polyacrylamide gels. The gels were stained with Coomassie brilliant blue R-250 and images captured by Pharos FX<sup>TM</sup> plus molecular imager scanner (BIO-RAD).

### 3.4 Summary

Protein extraction from pulp, fruit skin and leaf of the pear was optimized as shown in Figure 3.1. Proteome profiles were successfully established. However, sample preparation is a crucial step for obtaining reproducible and high resolution gels. The use of high quality protein samples and loading the correct protein concentration have demonstrated to be a key factor/step towards generating well resolved 2D proteome maps. Selection of the right pH scale/range for protein separation in 2D is of significant importance as this will help to improve the resolution of the 2D gels. The use of pure reagents remains a priority especially if down stream processing of protein spots is to be done. The use of chemicals that are not compatible with the mass spectrometry instruments should be avoided, as this tends to interfere and interact with the sensitivity of the instrument. Moreover, any solubilising agent used prior to IEF should not change the original *pI* of the proteins.







**CHAPTER 4**

**COMPARISON OF RED AND GREEN ‘BON ROUGE’  
PHENOTYPES AND PROTEIN IDENTIFICATION**

UNIVERSITY *of the*  
WESTERN CAPE

#### 4.1 Introduction

In Chapter 3, a description of the establishment of 2D proteome maps was given. Therefore, the objective of this chapter is to compare and analyse the proteome of both the red and green phenotypes of 'Bon Rouge' pear tree materials using their 2D proteome maps. The 'Bon Rouge' pear (red) and the 'Bon Rouge' revertant pear (green) are genetically closely related as one is the mutant of the other. During the past few years, the characterisation and the differentiation of genetic relationship between the species and cultivars was based solely on the use of molecular markers. Molecular markers are being widely used for fingerprinting cultivars of different fruit tree species (Wunsch and Hormaza, 2007).

However, in spite of those previously done studies, the information is still lacking on the molecular characterisation and estimation of the genetic variability of most European pear cultivars (Wunsch and Hormaza, 2007). Inoue *et al.*, (2006), stated the difficulty of conducting the early selection on the fruit phenotypes since the fruit crops have a long vegetation period and therefore, labour and costs tends to increase. In pears, any evaluation and selection of such fruit characteristics as skin colour, firmness, weight, sweetness, and acidity are impossible within a period of years until flowering and setting fruit at the F<sub>1</sub> progeny (Inoue *et al.*, 2006).

However, with the rapidly evolving field of proteomics and the development of new technologies such as mass spectrometry, the breeding efficiency could be improved. Proteomics is directed towards providing a comprehensive view of the characteristics and activities of every cellular protein under any growth stages and conditions. As a result proteomics application in breeding industry could reduce the long vegetation period, the

labour and the running costs as the fruit crops can be analysed at any given stage and condition of growth.

In this study comparative proteomics analysis was carried out on the fruit skins and the leaves of 'Bon Rouge' pear material. Two types of seedlings were used namely 'Bon Rouge' and the 'Bon Rouge' reverted phenotype. A total of twelve clones were also used. Six of the clones were of the 'Bon Rouge' origin and the other six were of 'Bon Rouge' reverted phenotypes.

The same effects have also been investigated in 'Bon Rouge' pear fruits using the same approach where by the fruit skins were separated from the pulp. The mature and ripen pear fruits skins were cut approximately 0.5 mm deep using a vegetable peeler, in order to maintain the consistency in their depth. Several fruit skins from pear fruits were combined together from both red sided and green sided pears respectively during the time of study in order to minimize the cost of high priced pears from the farms.

## **4.2 Results and Discussion**

### **4.2.1 1D SDS-PAGE of red and green 'Bon Rouge' phenotypes using their total soluble proteins (TSP)**

The protein samples from all the leaves and fruit skin materials were first analysed on a 12 % 1D SDS-PAGE following the protocol in Section 2.2.1.1 and 2.2.1.2 respectively. The results are presented in Figure 4.1 and Figure 4.2. In Figure 4.1 lane 1 shows molecular weight marker and lanes 2-9 shows leaf materials proteins, 'Bon Rouge', 'Bon Rouge' revertant, BR1, BRR1, BR7, BRR7, BR8, and BRR8 respectively and Figure 4.2 lane 1 shows molecular weight marker and lanes 2-7 show leaf material proteins, BR9, BRR9, BR16, BRR16, BR22 and BRR22 respectively. The experiment was performed to determine if there

is any similarity between the red ('Bon Rouge') and green ('Bon Rouge' revertant) leaves. The 1D SDS-PAGE of the TSP of pear leaves proteins displays similar banding pattern with the molecular weight ranging from 120 kDa to 10 kDa between both the red ('Bon Rouge') and green ('Bon Rouge' revertant) leaves in both Figure 4.1 and Figure 4.2 respectively. The most abundant proteins were observed between 85 kDa and 25 kDa with the ones just below 25 kDa appearing faint in both figures (Figure 4.1 and Figure 4.2). This observation emphasizes that there is great relatedness between red ('Bon Rouge') and green ('Bon Rouge' revertant) leaves from both clones and their parental seedlings.

However, the green ('Bon Rouge' revertant) leaves in both Figure 4.1 and Figure 4.2, appear to have an extra band with a molecular weight of approximately 53 kDa which appears to be less abundant in red ('Bon Rouge') leaves. This band appears to be the only differentiating factor between red ('Bon Rouge') and green ('Bon Rouge' revertant) leaves and at this stage it is not clear if this most abundant protein is the marker that confers the green ('Bon Rouge' revertant) leaves their green colour as it is found in green leaves.

The highlighted area in Figure 4.1 and Figure 4.2 respectively, shows the area where the major differences are observed between the red ('Bon Rouge') and green ('Bon Rouge' revertant) leaves of both the seedling and clones. However, the TSP between the BR7 (red wild type leaves) and BRR7 (green mutant leaves) clones in lanes 6 and 7 respectively, did not show any significant differences (Figure 4.1). Based on the observations made in other sets of leaves (Table 2.1) more especially the green leaves, it could be postulated that the BRR7 (green mutant leaves) have lost that differential marker, which distinguishes the red (wild type leaves) leaves from the green (mutant leaves) ones.

#### 4.2.2 2D-PAGE of red and green 'Bon Rouge' phenotypes

Following the 1D SDS-PAGE success, the proteins were separated on the first dimensional using the IPG strips (Section 2.2.5.2). The choice of IPG strip length and pH range was based on the information obtained during the successful establishment of 2D proteome profiles in Section 3.3. The IPG strips of this length and pH range (7 cm, pH 4-7, BIO-RAD) were used and they gave maximum spot resolution in all the pear tissues analysed (as seen in Figure 3.3).

It was observed in the 2D gels that the majority of protein spots had a *pI* ranges between 4 and 7, with the molecular weight ranging between 10 kDa and 120 kDa in all the tissues analysed. The 2D gels demonstrated and reaffirmed that individual proteins are separated differently between tissues, despite tissues being from the same plants. The green leaf materials had an extra protein spot running at approximately 53 kDa. Figure 4.3B shows this differential spot (spot number 7), and this spot was either missing or less abundant in the red leaves (Figure 4.3A). The spot had the molecular weight that resembles the one observed in the 1D SDS-PAGE running at approximately 53 kDa.

The majority of protein spots were found to be reproducible between both gels in Figure 4.3A and Figure 4.3B respectively. Contrary to the faint bands below the molecular weight of 25 kDa observed on 1D SDS-PAGE, there was several well resolved and high-abundant protein spots running below this molecular weight of 25 kDa as observed on 2D profiles both on Figure 4.3A and 4.3B respectively. Figure 4.3B shows the proteins spots that were taken for further analysis and they are indicated with arrows numbered 1-10. The differential protein spot was included and was numbered 7 on Figure 4.3B.



**Figure 4.1** 1D SDS-PAGE profiles of pear leaf TSP. Approximately 20 µg of pear tree leaf protein samples were separated on 12 % SDS polyacrylamide gel. The gels were stained with Coomassie brilliant blue R-250 and images captured by Pharos FX™ plus molecular imager scanner (BIO-RAD).



**Figure 4.2** 1D SDS-PAGE profiles of pear leaf TSP. Approximately 20  $\mu\text{g}$  of pear tree leaf protein samples were separated on a 12 % SDS polyacrylamide gel. The gels were stained with Coomassie brilliant blue R-250 and images captured by Pharos FX<sup>TM</sup> plus molecular imager scanner (BIO-RAD).

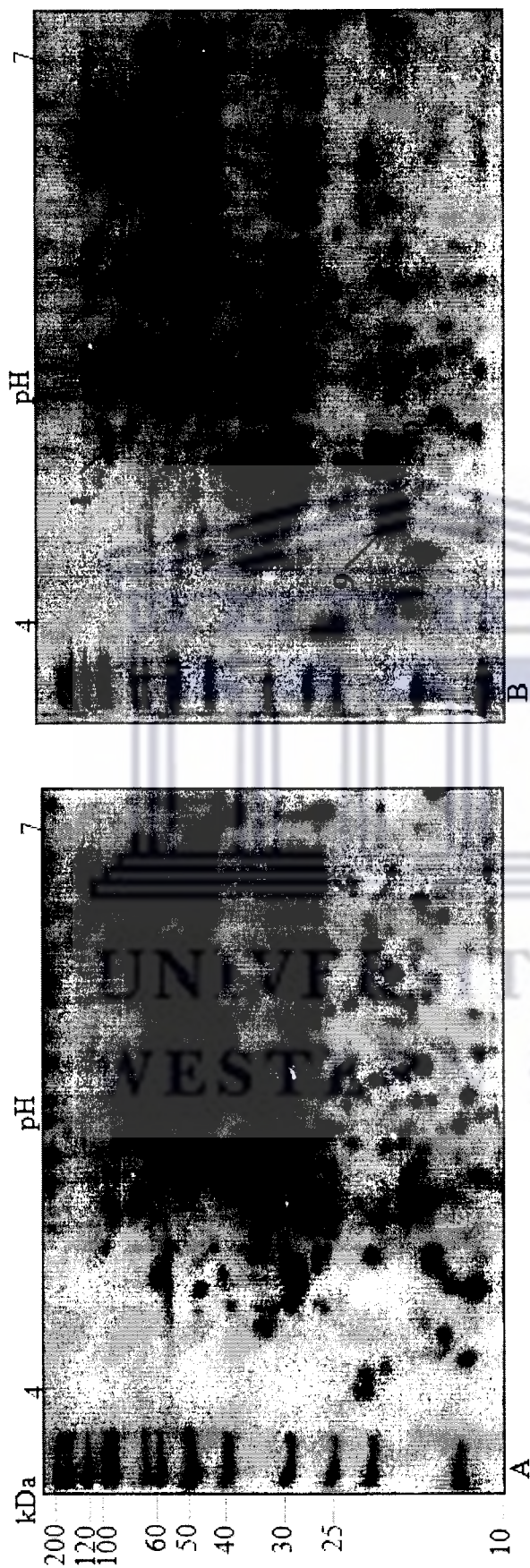


**Figure 4.3** Comparative 2D profiles of 'Bon Rouge' and 'Bon Rouge' revertant using their TSP (A) 'Bon Rouge' and (B) 'Bon Rouge' revertant. Arrows and numbers in Figure B, indicate the protein spots which were picked and identified by MALDI-TOF-MS (Applied Biosciences). The highlighted area on the 2D gels indicates the differential spot which is absent or less expressed in 'Bon Rouge'. Approximately 150  $\mu\text{g}$  of leaf protein sample was isoelectric-focused on a 7 cm IPG strips (pH 4-7, BIO-RAD) and then separated in the second dimension on a 12 % SDS polyacrylamide gels. The gels were stained with Coomassie brilliant blue R-250 and images captured by Phoros FX™ plus molecular imager scanner (BIO-RAD).



### 4.2.3 Protein identification

Following the successful separation of protein spots in 2D profiles in Figure 4.3A and Figure 4.3B, ten abundant protein spots were excised from the 2D gel for further analysis with MALDI-TOF-MS (Applied Biosciences). As already mentioned, the spots were indicated by arrows and were numbered 1-10 as indicated in Figure 4.3B. The excised protein spots were digested with trypsin (Section 2.2.6) and the resulting peptide fragments were extracted and identified by peptide mass fingerprinting using a MALDI-TOF-MS. (Applied Biosciences).

Out of ten proteins spots five proteins spots numbered 3, 4, 5, 6, and 7 in Figure 4.3B were successfully identified with a significantly high mouse score which is calculated as  $-10 \times \log_{10}(P)$ , where P is the absolute probability that observed matched is a random event. Thus, the higher score indicates identity on extensive homology of the unknown protein with the identified one.

Spot number 3 in Figure 4.3B was identified as PAL from the database. This protein was identified with significant mouse score of 66. The theoretical molecular weight and pI value of this protein were 52 kDa and 5.73 respectively as compared to the estimated molecular weight of 50 kDa and pI 5.1 from the gels.

Spots numbers 3 and 4 were both identified as Photosystem II protein in Figure 4.3B. This two protein spots were identified with significant score of 79 and 75 respectively. When comparing their theoretical and actual molecular weights and pI are compared very little difference could be noticed.

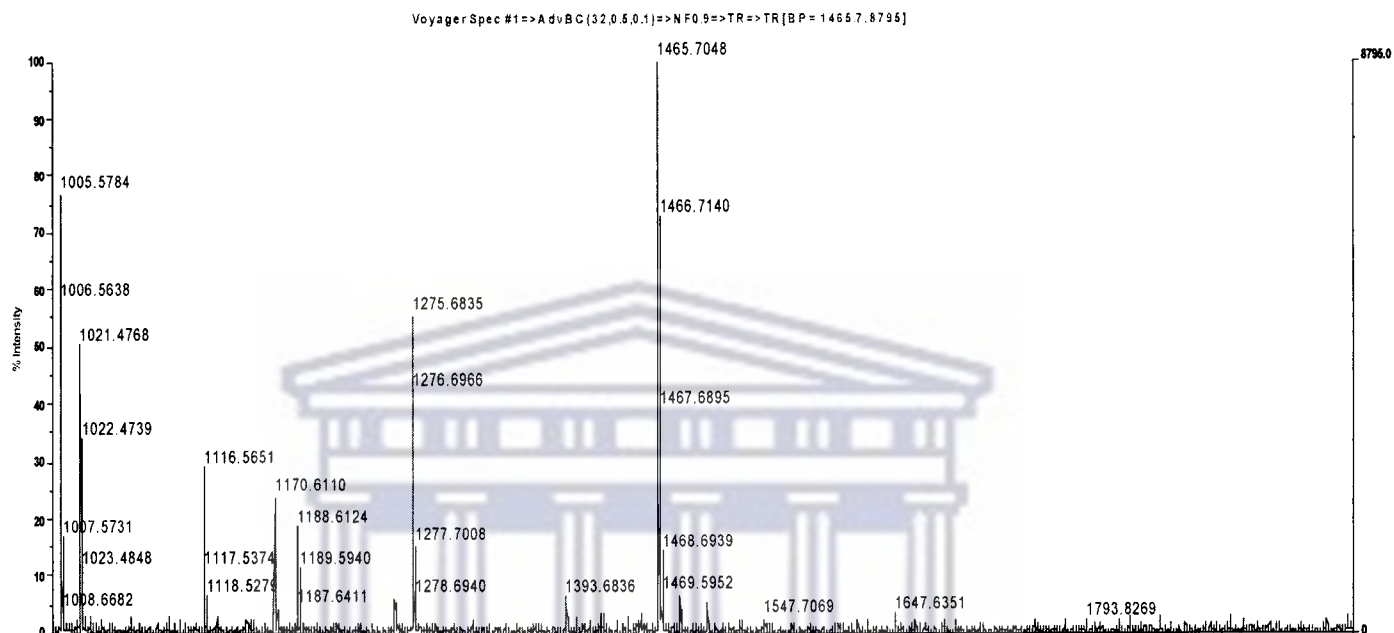
Spots numbers 6 and 7 in Figure 4.3B, appear as a two co-migrating spots as it was observed in the green ('Bon Rouge' revertant) leaves only. This spot complex was identified as RuBisCO large subunit, spot number 6 with significant score of 66 whereas spot number 7 had a highest significant score of 100. When comparing their theoretical molecular weights and *pI*, between this two spots there was very little difference.

Figure 4.4B, shows an example of an identified protein and Figure 4.4A represents MALDI-TOF-MS ion spectrum of a fragmented ions of a peptide from protein spot number 7 (Figure 4.3B), which was identified as RuBisCO large sub-unit and ions scores of identified peptides were significantly high enough for the peptide to be accepted. All the identified proteins are summarized in Table 4.1 with protein name, Mowse score, molecular weight from database, *pI* from database, molecular weight from gel and *pI* from gel.

The identification of the 53 kDa protein as a large subunit of ribulose-1,5-bisphosphate carboxylase/oxygenase (RuBisCO) by MALDI-TOF-MS (Applied Biosciences) have correlated with previous studies conducted on higher plants. RuBisCO has been well researched in higher plants and it was found to be the most abundant protein in plant leaves occupying about fifty percents of soluble proteins in leaves. This protein executes most of the photosynthetic and respiratory activities in green higher plants. The absence of this protein spot (RuBisCO large subunit) in the red leaves of 'Bon Rouge' pear leaves could be attributed to the fact that red colouration in most cases in plants is associated with stress. Plants under stressful conditions produce high amounts anthocyanins and it is enhanced by

the presence of factors such as light. Light is the source of energy for photosynthesis and too much of it also could be harmful to plants.

A.



B.

GTGFKAGVKD YKLTYYTPEY ATKDTDILAA FRVTPQPGVP PEEAGAAVAA  
 ESSTGTWTTV WTDGLTSLDR YKGRCYGIEP VAGEENQFIA YVAYPLDLFE  
 EGSVTNMFTS IVGNVFGFKA LRALRLEDLR IPPAYVKTFQ **GPPHGIQVER**  
 DKLNKYGRPL LGCTIKPKLG LSAKNYGRAV YECLRGGLDF TKDDENVNSQ  
 PFMRWRDRFL FCAEAIYKAQ AETGEIKGHY LNATAGTCEE MIKRAVFARE  
 LGVPIVMHDY LTGGFTANTS LAHYCRDNGL LLHIHRAMHA VIDRQKNHGI  
 HFRVLAKRLR **MSGGDHIHSG TVVGKLEGER EITLGFVDLL RDDYIEKDRS**  
 RGIYFTQDWV SLPGVLPVAS GGIHVWHMPA LTEIFGDDSV LQFGGGTLGH  
 PWGNAPGAVA NRVALEACVQ ARNEGRDLAC **KGNEIIREASWSPELAAAC**  
 EVWKEIKFEF EAMDTL

**Figure 4.4** MALDI-TOF-MS ion spectrum of Ribulose 1,5-biphosphate carboxylase large subunit (**AAA82565**). Spot 7 (Figure 4.3B) was cut from the gel and digested with trypsin. The tryptic digests were analysed with MALDI-TOF-MS (Applied Biosciences) and the detected spectrum is shown in (A), (B) The identified polypeptide and the peptide coverage is shown (bold). The summary of other identified proteins is shown in Table 4.1.

**Table 4.1:** Summary of the protein spots identified by MALDI-TOF-MS (Applied Biosciences) from 2D gel in Figure 4.3B

Protein spot number	Name of protein identified	Mowse score	Molecular weight from database (kDa)	pI from database	Molecular weight from gel (kDa)	pI from the gel
1	NI					
2	NI					
3	Phenyl alanine ammonia-lyase	66	52 204	5.73	50 000	5.1
4	Putative 33kDa oxygen evolving protein of photosystem II	79	34 840	5.89	35 000	5.3
5	Photosystem II oxygen evolving complex protein I	75	35 236	5.87	35 000	5.4
6	Ribulose 1,5-bis phosphate carboxylase oxygenase large subunit	66	51 644	6.23	52 000	6.4
7	Ribulose 1,5-bis phosphate carboxylase oxygenase large subunit	100	51 666	6.31	52 000	6.5
8	NI					
9	NI					
10	NI					

NI-Not identified

### 4.3 Comparative analysis of proteins profiles of pear leaf clones and fruit skin

A total of 14 2D gels were completed in this section for comparative analysis. The gels consisted of two 2D gels from fruit skin (red and green) and six pairs of pear clones to determine whether they exhibit the same expression profiles as their parents ('Bon Rouge' pear and 'Bon Rouge' revertant pear leaves). The clone pairs consisted of BR1, BRR1; BR7, BRR7; BR8, BRR8; BR9, BRR9; BR16, BRR16; BR22, BRR22. Protein spots were reproducibly resolved across all the 12 gels (Figure 4.5.1 – Figure 4.5.6), resulting in similar protein spot locations across the spectrum, where by the clones followed the same 2D profiles as their parental seedling leaves.

The experiment was repeated several times using different biological replicates from the same clones to confirm the exact positions of the protein spots. The differentially induced spot was observed in 2D gels of clones as it was seen in the seedling. However, the protein spots were not identified as the aim of this section was to verify if there is any correlation between the clones and the seedling using their 2D profiles. On the other hand the fruit skins were compared amongst themselves. The 2D profiles of both red and green pears skins appear to be very similar to each other, with the majority of proteins having molecular weight ranging between 100 kDa and 15 kDa. It was observed that pear skins proteins were dominated by low abundance proteins spots appearing in a straight line between the molecular range of 100 kDa and 40 kDa. The proteins profile of green skin 2D appears to be slightly over expressed as compared to their red counterpart. Generally, the fruit skins were found to have fewer proteins spots as compared to the leaf proteome.

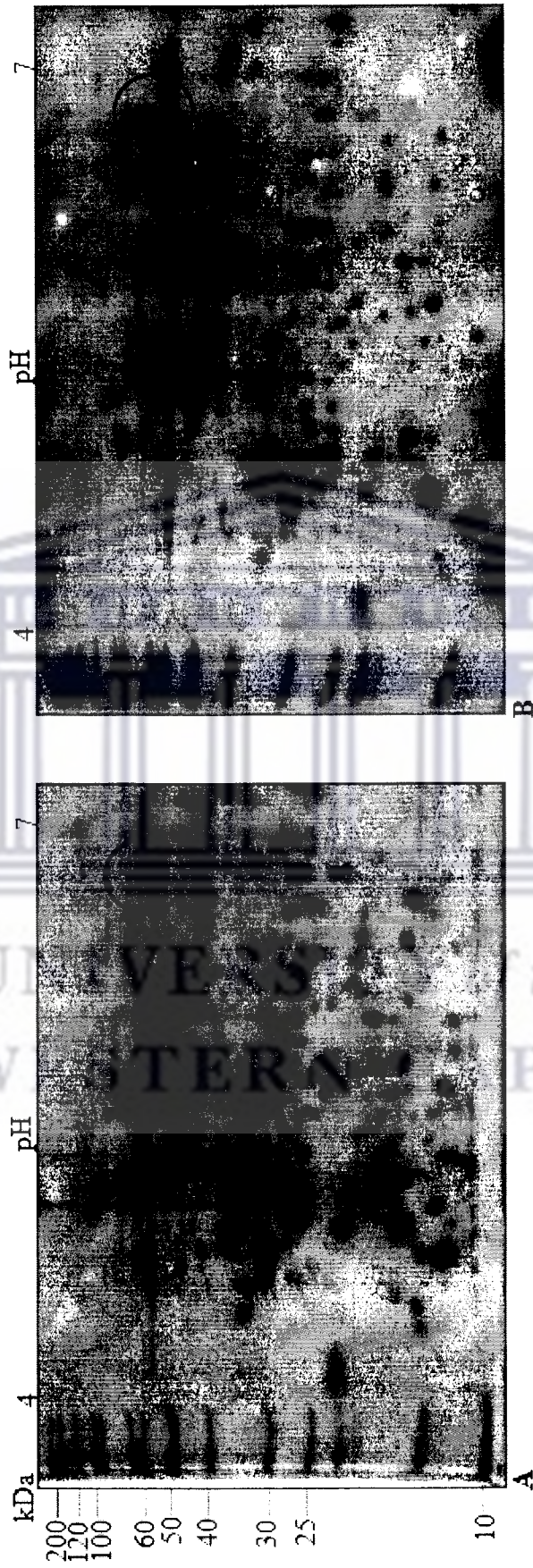


**Figure 4.5.1** Comparative 2D profiles of pear leaf total soluble proteins from pear clones (A) BR1 and (B) BRR1. The highlighted area on the 2D gels indicate the differential spot which is absent or less expressed in clone BR1. Approximately 150  $\mu\text{g}$  of leaf protein sample was isoelectric-focused on a 7 cm IPG strips (pH 4-7, BIO-RAD) and then separated in the second dimension on a 12 % SDS polyacrylamide gel. The gels were stained with Coomassie brilliant blue R-250 and imaged captured by Phoros FX™ plus molecular imager scanner (BIO-RAD).



**Figure 4.5.2** Comparative 2D profiles of pear leaf total soluble proteins from pear clones (A) BR7 and (B) BRR7. The highlighted area on the 2D gels indicate the differential spot which is absent or less expressed in clone BR7. Approximately 150  $\mu$ g of leaf protein sample was isoelectric-focused on a 7 cm IPG strips (pH 4-7, BIO-RAD) and then separated in the second dimension on a 12 % SDS polyacrylamide gel. The gels were stained with Coomassie brilliant blue R-250 and images captured by Phoros FX<sup>TM</sup> plus molecular imager scanner (BIO-RAD).



**Figure 4.5.3** Comparative 2D profiles of pear leaf total soluble proteins from pear clones (A) BR8 and (B) BRR8. The highlighted area on the 2D gels indicates the differential spot which is absent or less expressed in clone BR8. Approximately 150 µg of leaf protein sample was isoelectric-focused on a 7 cm IPG strips (pH 4-7, BIO-RAD) and then separated in the second dimension on a 12 % SDS polyacrylamide gel. The gels were stained with Coomassie brilliant blue R-250 and images captured by Phoros FX™ plus molecular imager scanner (BIO-RAD).



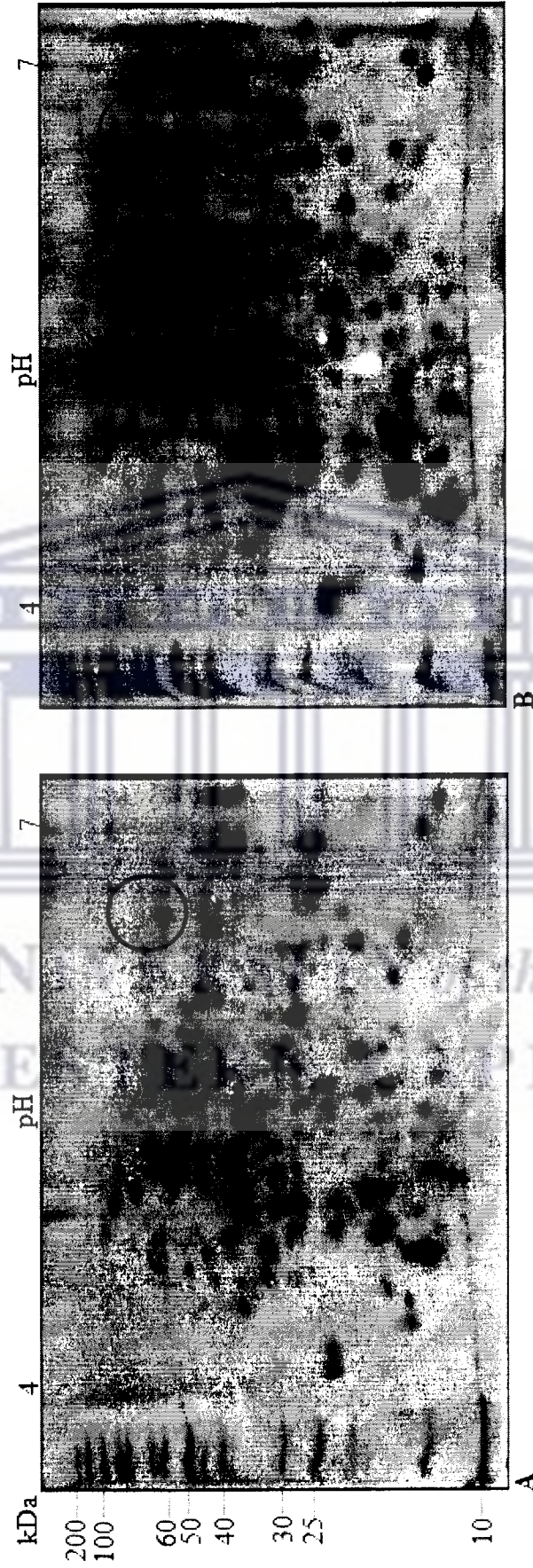


**Figure 4.5.4** Comparative 2D profiles of pear leaf total soluble proteins from pear clones (A) BR9 and (B) BRR9. The highlighted area on the 2D gels indicate the differential spot which is absent or less expressed in clone BR9. Approximately 150  $\mu\text{g}$  of leaf protein sample was isoelectric-focused on a 7 cm IPG strips (pH 4-7, BIO-RAD) and then separated in the second dimension on a 12 % SDS polyacrylamide gel. The gels were stained with Coomassie brilliant blue R-250 and images captured by Pharos FX<sup>TM</sup> plus molecular imager scanner (BIO-RAD).

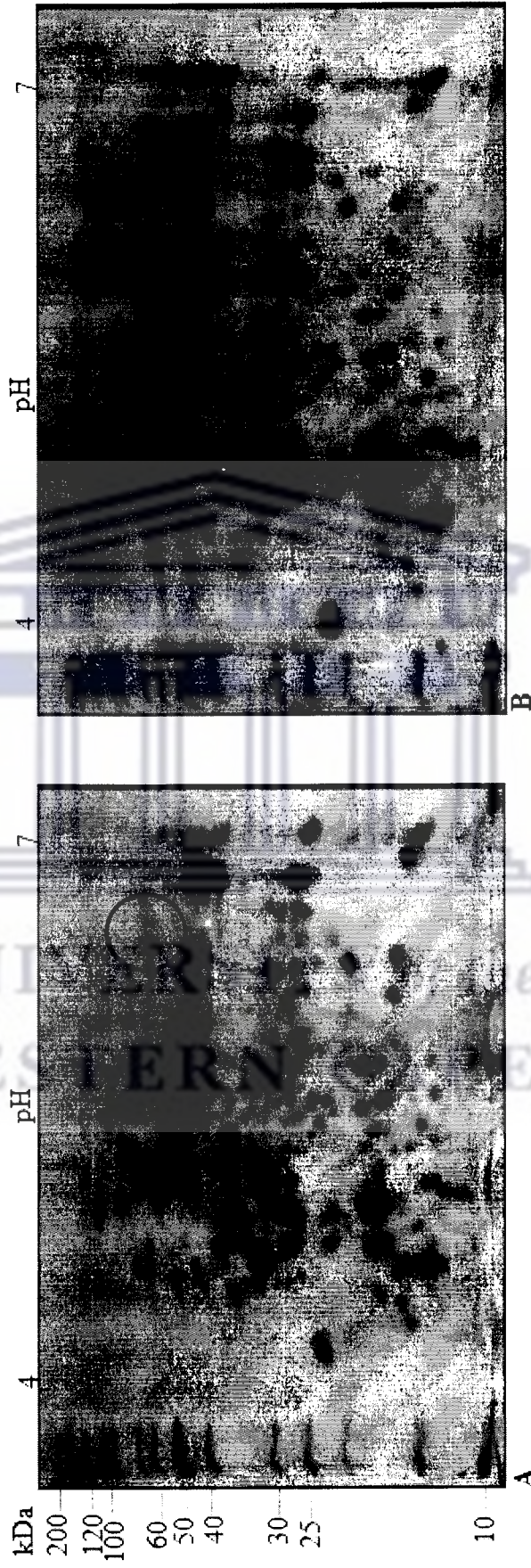


**Figure 4.5.5** Comparative 2D profiles of pear leaf total soluble proteins from pear clones **(A)** BR16 and **(B)** BRR16. The highlighted area on the 2D gels indicates the differential spot which is absent or less expressed in clone BRR16. Approximately 150  $\mu\text{g}$  of leaf protein sample was isoelectric-focused on a 7 cm IPG strips (pH 4-7, BIO-RAD) and then separated in the second dimension on a 12 % SDS polyacrylamide gel. The gels were stained with Coomassie brilliant blue R-250 and images captured by Phoros FX<sup>TM</sup> plus molecular imager scanner (BIO-RAD).



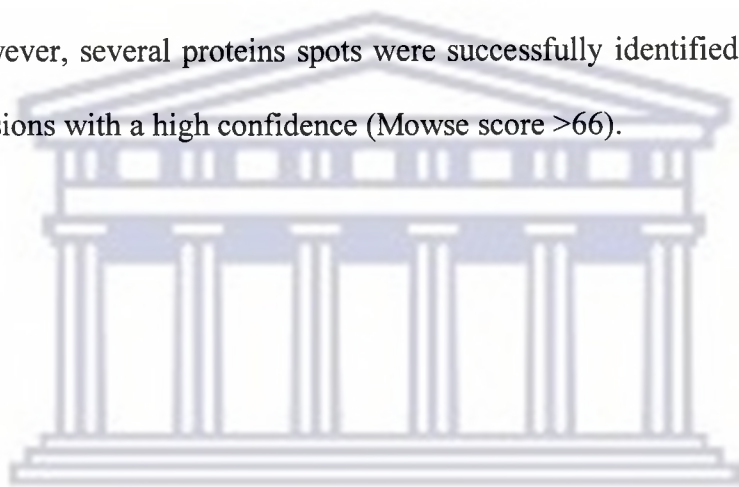
**Figure 4.5.6** Comparative 2D profiles of pear leaf total soluble proteins from pear clones (A) BR22 and (B) BRR22. The highlighted area on the 2D gels indicates the differential spot which is absent or less expressed in clone BR22. Approximately 150  $\mu\text{g}$  of leaf protein sample was isoelectric-focused on a 7 cm IPG strips (pH 4-7, BIO-RAD) and then separated in the second dimension on a 12 % SDS polyacrylamide gel. The gels were stained with Coomassie brilliant blue R-250 and images captured by Phoros FX<sup>TM</sup> plus molecular imager scanner (BIO-RAD).



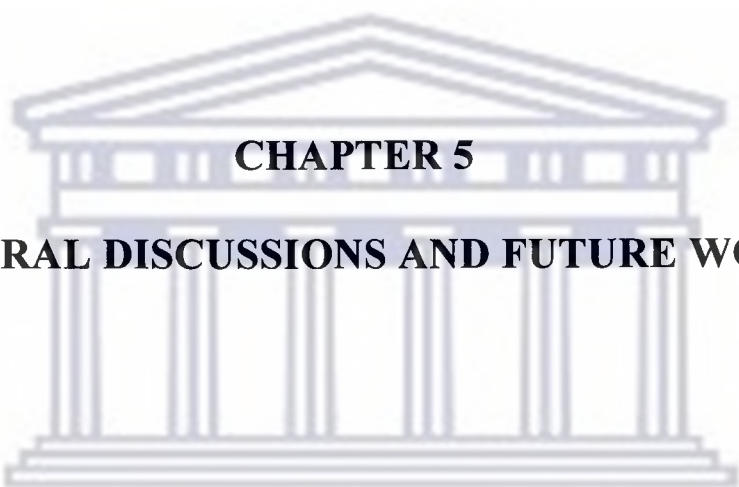
**Figure 4.6** Comparative 2D gels profiles of pear fruit skin samples using their TSP, (A) red skin and (B) green skin. Approximately 150  $\mu\text{g}$  of fruit skin protein sample was isoelectric-focused on a 7 cm IPG strips (pH 4-7, BIO-RAD) and then separated in the second dimension on a 12 % SDS polyacrylamide gel. The gels were stained with Coomassie brilliant blue R-250 and images captured by Phoros FX™ plus molecular imager scanner (BIO-RAD).

#### 4.4 Summary

Replicates of 2D gels were analysed from different biological replicates and protein spots were reproducible in all the replicates. The differential protein spots were seen on the gels without the assistance of any software that are used when no differences could be spotted. The resultant differential protein spots between the 'Bon Rouge' and 'Bon Rouge' revertant leaves and high abundant proteins spots were excised from the gels for identification by MALDI-TOF-MS. This analysis did not include low abundance proteins spots because of the anticipated difficulties in obtaining the satisfactory protein identification by mass spectrometry. However, several proteins spots were successfully identified and reconfirmed on numerous occasions with a high confidence (Mowse score >66).



UNIVERSITY *of the*  
WESTERN CAPE

The logo of the University of the Western Cape, featuring a classical building facade with a pediment and six columns.

**CHAPTER 5**  
**GENERAL DISCUSSIONS AND FUTURE WORK**

UNIVERSITY *of the*  
WESTERN CAPE

The main aims of this study were to generate and construct first 2D proteome spot profiles and identify the differential proteins between the red and green 'Bon Rouge' phenotypes using the proteomics approach. As far as it stands the proteomic approach have delivered the desired results as this was the first attempt ever to map the pear fruit tissues. Thus far it has proven to be possible. This study have demonstrated the role which proteomics application could play in differentiating most fruit crops species, more especially in the breeding industry. This approach might not necessarily have given all the solutions to the challenges the breeding industry is faced with but it has laid a solid foundation for plant proteomics research.

Out of 10 spots analysed by MALDI-TOF-MS (Applied Biosciences), on the mini gels upon Coomassie staining 5 spots gave positive identification (Figure 4.3B, spots numbers 3-7) and the other 5 spots did not give positive identity (Figure 4.3B, spots numbers 1, 2, 8, 9, and 10). These identified proteins spots appear to be highly conserved proteins in higher plants and seem to play important roles in a leaf energy metabolism.

Briefly, spots numbers 6 and 7, Figure 4.3B were identified as RuBisCO. RuBisCO is the primary enzyme in photosynthetic carbon fixation (Xu *et al.*, 2006). The other equally important protein spots identified here are Photosystem II complex proteins (Putative 33kDa oxygen evolving protein of Photosystem II and Photosystem II oxygen evolving complex protein I, spots numbers 4 and 5 respectively, Figure 4.3B). Photosystem II is the light harvesting complex and it is highly abundant protein in thylakoid membrane of plant chloroplast. As already mentioned in Section 1.10.1, the functions of Phenylalanine ammonia-lyase (PAL) is the first enzyme that catalyses the first committed step in the

biosynthesis of phenylpropanoids, which performs a variety of functions in plant development and in plant interaction with the environment (Shufflebottom *et al.*, 1993).

The main function of plant leaf is energy harvesting, conversion and storage. Therefore it is not surprising that the proteins identified here have important function related to energy metabolism in leaves. However, due to the number of environmental factors such as light, the leaves end up not being able to meet the demand of energy capturing, storage and dissipating and as a result the stressful condition will occur.

During the comparative analysis between the red ('Bon Rouge') and green ('Bon Rouge' revertant) leaves of 'Bon Rouge', it was observed that red leaves do not produce or produce very little RuBisCO, which is therefore difficult for the leaves to cope with high demand of photosynthesis. This idea is further supported by the absence of this protein on the skin proteins which means it is a green leaf specific protein. Based on the observation made it is clear that the red colouration on the leaves of is due to light stress. Zhang *et al.*, (2005) reported the degradation of RuBisCO in wheat leaves by light stress even though no colour change was reported. However, it would be interesting to establish the roles and mechanisms that RuBisCO uses in the green colour formation, as it is seen already that RuBisCO is implicated in colour formation.

On the other hand, the light-induced damage is also believed to be targeted mainly to photosystem II protein complex and this type of damage leads to an inactivation of electron transport and subsequent oxidative damage of the reaction centre, in particular the D<sub>1</sub> protein. Aro *et al.*, (1993), proposed the mechanisms in which inactivation and protein damage can be effected either from the acceptor side or donor side of p680. They stated that the damaged D<sub>1</sub>



protein is triggered for degradation and digestion by at least one serine-type proteinase that is tightly associated with photosystem II complex itself. The damaged photosystem II complex dissociates from the light harvesting antenna and migrates from appressed to non-appressed thylakoid region where a new D<sub>1</sub> protein is co-translationally inserted into the partially disassembled photosystem II complex. D<sub>1</sub> proteins allows for coordinated biodegradation and biosynthesis of the D<sub>1</sub> protein. After realignment of cofactors and assembly of subunits, the repaired photosystem II complex can again be found in the appressed membranes regions. This could be the possible reason why anthocyanin appears transiently and suddenly disappears as soon as conditions turn to be more favourable. Some of the leaves particularly the older ones may start falling off from the trees as a result of failure to recover from this photoinhibitory damage occurred on them and their inability to cope with high demand of photosynthetic processes.

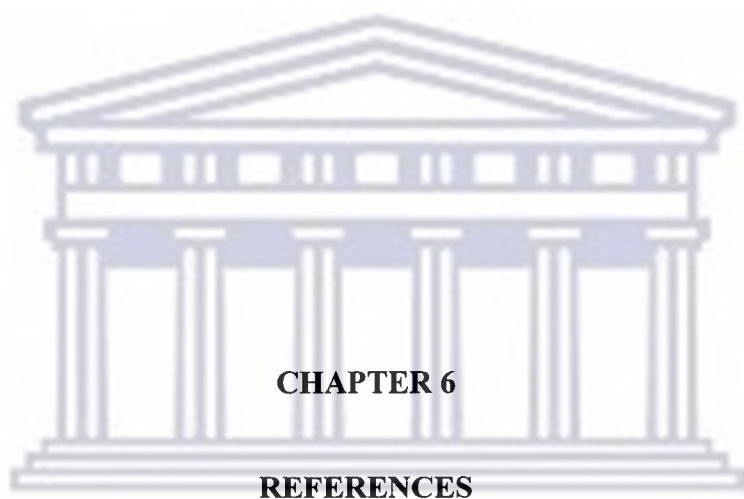
The unidentified proteins did not match anything from the MSDB. These unidentified proteins had low ion scores below the normal threshold, therefore implying that the match occurred randomly. The failure to match anything from available databases could be attributed to the absence of pear specific database. Proteins with a full length sequence present in databases will be identified with high certainty and high throughput using the accurate masses obtained from MALDI-TOF-MS peptide mapping (Encarnacion *et al.*, 2005). The availability of complete genome sequence of genus *Pyrus* and the erection of pome fruit crops protein database will be of a significance importance in identifying protein involved in various cellular activities.

However, once the complete genome sequence of pears becomes available, it will be possible and easy to identify most proteins with high accuracy. The very same spectrums that did not give any positive identity can still be used to search for identity of those spots with an

outstanding identity. It will be interesting to know which proteins the spectrum matches in the database and as well as to establish whether they are known protein with known functions. Thus would be interesting even more if the spectrum matches the novel proteins. The sooner the complete genome sequence becomes available it will enable the researches to map all the proteins available from the pear genome and be able compare them with the proteins from other plants. It will be good to know how proteins from various tissues are related in terms of their structures, functions and as well as their biological pathways. This could be done on tissue to tissue or across various plants species.

In conclusion, handling and preparation of protein samples from plant materials hold the key to the 2D reference maps success and could be of interest to the laboratories involved in plant proteomics. The plant tissues are susceptible to contamination and are fast to oxidise. These factors should be avoided during sample preparation especially if downstream processing of protein spots is to be done. Contaminants and impurities could be detected by mass spectrometry and their presence could have a negative impact on the protein identifications and will heavily alter the results. The key elements in the success of 2D include the extraction and the detection of as many proteins as possible whilst minimizing the post extraction artefacts, comparison of samples, protein identification.

Fruit crops are seasonal and as such the researches are forced to wait too long or keep their plant tissues under the freezing conditions for prolonged period in order to keep with constant supply while plants are in their dormancy stage. As such, in future the approach might be to introduce the tissue culture system. This approach will help to keep the constant supply of the tissues of interest and as well as to ensure that this tissues are under the stringent controlled conditions to monitor the cellular changes.



**CHAPTER 6**

**REFERENCES**

UNIVERSITY *of the*  
WESTERN CAPE

**Aebersold, R., and Matthias, M. (2003).** Mass spectrometry based proteomics. *Nature*. 422: 198-207.

**Aro, E. M., Virgin, I., Andersson, B. (1993).** Photoinhibition of photosystem II. Inactivation, protein damage and turnover. *Biochim Biophys Acta*. 1143(2): 113-134.

**Barbier-Brygoo, H., and Joyard, J. (2004).** Focus on plant proteomics. *Plant Physiology and Biochemistry*. 42: 913-917.

**Beranova-Giorgianni, S. (2003).** Proteome analysis by two-dimensional gel electrophoresis and mass spectrometry: strengths and limitations. *Trends in analytical chemistry*. 22(5): 273.

**Bhadauria, V., Zhao, W., Wang, L., Zhang, Y., Liu, J., Yang, J., Kong, L., and Peng, Y. (2007).** Advances in fungal proteomics. *Microbiological research*. 162: 193-200.

**Booi, S., van Dyk, M. M., du Preez, M. G., and Rees, D. J. G. (2005).** Molecular typing of red and green phenotypes of 'Bon Rouge' pear trees, with the use of microsatellites. *Acta Horticulturae*. 671: 293.

**Bradford, M. M. (1976).** A rapid and sensitive method for the quantification of microgram quantities of protein utilizing the principle of protein-dye binding. *Analytical biochemistry*. 72: 248-254.

**Bruce, T. J. A., and Pickett, J. A. (2007).** Plants defence signalling induced by biotic attacks. *Current opinion in plant Biology*. 10: 387-392.

**Chalker-Scott, L. (1999).** Environmental significance of anthocyanins in plant stress responses. *Photochemistry and photobiology*. 1: 1.

**Close, D. C., and Beadle, C. L. (2003).** The ecophysiology of foliar anthocyanin. *The botanical review*. 69(2): 149-161.

**Cooper-Driver, G. A. (2001).** Contribution of Jeffrey Harbone and co-workers to the study of anthocyanins. *Phytochemistry*. 56: 229-236.

**Di Michele, M., Chiatante, D., Plomion, C., and Scippa, G. S. (2006).** A proteomic analysis of Spanish broom (*Spartium junceum* L.) root growing on a slope condition. *Plant Science*. 170: 926-935.

**du Preez, M. G., and Rees, D. J. G. (2005).** Stress induced differential gene expression patterns for red and green phenotypes of 'Bon Rouge' pear trees (*Pyrus communis*). *Acta Horticulturae*. 671: 299.

**Dzhangaliev, A. D., Salova, T. N., and Turekhanova P. M. (2003).** The world fruit and nut plants of Kazakhstan. *Horticultural Reviews*. 29: 311.

**Encarnacion, S., Hernandez, M., Martinez-Batallar, G., Contreras, S., del Carmen Vargas, M., and Mora, J. (2005).** Comparative proteomics using 2D gel electrophoresis and mass spectrometry as tools to dissect stimulons and regulons in bacteria with sequenced or partially sequenced genomes. *Biological procedure online*. 7(1): 117-135.

**Feild, T. S., Lee, D. W., and Holbrook, N. M. (2001).** Why leaves turn red in autumn. The role of anthocyanins in senescing leaves of red-osier dogwood. *Plant Physiology*. 127: 566-574.

**Ferrandi, C. H., van der Merwe, P. W., and Huysamer, M. (2005).** Status of the pear industry in Africa, with specific reference to South Africa. *ACTA Horticulturae*. 671: 73-75.

**Gamble, J., Jaeger, S. R., and Harker, F. R. (2006).** Preferences in pear appearance and response to novelty among Australian and New Zealand consumers. *Postharvest biology and technology*. 41: 38-47.

**Garfin, D. E. (2003).** Two-dimensional gel electrophoresis: an overview. Trends in Analytical Chemistry. 22(5): 263.

**Gorg, A., and Weiss, W. (2004).** Proteome analysis: Interpreting the genome. First edition. Elsevier. USA. Pages 58-60.

**Heazlewood, J. L., and Millar, A. H. (2006).** Plant proteomics: challenges and resources. Blackwell publishing. 28: 2-3

**Holcroft, D. M., and Kader, A. A. (1999).** Carbon dioxide induced changes in color and anthocyanin synthesis of stored strawberry fruit. Hortscience. 34(7): 1244-1248.

**Holton, T. A., and Cornish, E. C. (1995).** Genetics and biochemistry of anthocyanin biosynthesis. The plant cell. 7: 1071-1083.

**Hood, B. L., Veenstra, T. D., and Conrads, T. P. (2004).** Mass spectrometry-based proteomics. International congress series. 1266: 375-380.

**Human, J. P. (2005).** Progress and challenges of the South Africa pear breeding program. ACTA Horticulturae. 671: 186-188.

**Inoue, E., Kasumi, M., Sakuma, F., Anzai, H., Amano, K., and Hara, H. (2006).** Identification of RAPD marker linked to fruit colour in Japanese pear (*Pyrus Pyrifolia* Nakai). Scientia Horticulturae. 107: 254-258.

**Jeong, S. T., Goto-Yamamoto, N., Kobayashi, S., and Esaka, M. (2004).** Effects of plants hormones and shading on the accumulation of anthocyanins and the expression of anthocyanin biosynthetic genes in grape berry skins. Plant science. 167: 247-252.

**Katterman, F. (1990).** Environmental injury to plants. First edition. Academic press. New York. p261.

**Kim, S., Lee, J., Hong, S., Yoo, Y., An, G., and Kim, S. R. (2003).** Molecular cloning and analysis of anthocyanin biosynthesis genes preferentially expressed in apple skin. *Plant science*. 165: 403-413.

**Kong, J., Chia, L., Goh, N., Chia, T., and Brouillard, R. (2003).** Analysis and biological activities of anthocyanins. *Phytochemistry*. 64: 923-933.

**Laemmli, U. K. (1970).** Cleavage of structural proteins during the assembly of the head of bacteriophage T4. *Nature*. 227(5259): 680-685.

**Leyva, A., Jarillo, J. A. J., Salinas, J., and Martinez-Zapater, J. M. (1995).** Low temperature induces accumulation of phenylalanine ammonia-lyase and chalcone synthase mRNA of *Arabidopsis thaliana* in a light-dependent manner. *Plant physiology*. 108: 39-46.

**Lo Piero, A. R., Consoli, A., Puglisi, I., Orestano, G., Recupero, G. R., and Petrone, G. (2005).** Anthocyaninless cultivars of sweet oranges lack to express the UPD-Glucose flavonoid 3-O-Glucosyl transferase. *Plant biochemistry and biotechnology*. 14: 9-14.

**Lu, Q., and Yang, Q. (2006).** cDNA cloning and expression of anthocyanin biosynthetic genes in wild potato (*Solanum Pinnatisectum*). *African journal of biotechnology*. 5(10): 811-818.

**Ma, W., and Berkowitz, G. A. (2007).** The greatful dead: calcium and cell death in plant innate immunity. *Cellular microbiology*. 9(11): 2571-2585.

**Malcolm, P. (2006).** History of the pear. *Ezine articles*.1:1.

**Manetas Y. (2005).** Why some leaves are anthocyanic and why most anthocyanic leaves are red? *Flora*. 201: 163-177.

**Merzlyak, M. N., and Chivkunoa, O. B. (2000).** Light-stress-induced pigment changes and evidence for anthocyanin photoprotection in apples. *Journal of photochemistry and photobiology.* 55: 155-163.

**Monte-Corvo, L., Cabrita, L., Oliveira, C., and Leitao, J. (2000).** Assessment of genetic relationships among *Pyrus* species and cultivars using AFLP and RAPD markers. *Genetic resources and crop evolution.* 47: 257-265.

**Munne-Bosch, S., and Alegre, L. (2004).** Die and let live: leaf senescence contributes to plant survival under drought stress. *Functional plant biology.* 31: 203-216.

**Ndimba, B. K., Chivasa, S., Hamilton, J. M., Simon, W. J., and Slabas, A. R. (2003).** Proteomics analysis of changes in the extracellular matrix of *Arabidopsis* cell suspension cultures induced by fungal elicitors. *Proteomics.* 3:1047-1059.

**Oliveira, C. M., Mota, L., Monte-Corvo, L., Goulao, L., and Silva, D. M. (1999).** Molecular typing of *Pyrus* based on RAPD markers. *Scientia Horticulturae* 79: 163-174.

**Park, O. K. (2004).** Proteomic studies in plants. *Journal of biochemistry and molecular Biology.* 37: 133-138.

**Patterson, S. D., and Aebersold, R. H. (2003).** Proteomics: the first decade and beyond. *Nature genetic supplement.* 33: 311.

**Pirondini, A., Visioli, G., Malcevski, A., and Marmioli, N. (2006).** A 2-D liquid-phase chromatography for proteomic analysis in plants tissues. *Journal of chromatography B.* 833: 91-100.

**Robinson, G. M., and Robinson, R. (1931).** A survey of anthocyanins. *Biochem.* 1: 1688-1705.



**Rose, J. K. C., Bashir, S., Giovannoni, J. J., Jahn, M. M., and Saravanan, R. S. (2004).** Tackling the plant proteome: practical approaches, hurdles and experimental tools. *The plant Journal*. 39: 715-733.

**Sanchez, E., Soto, J. M., Garcia, P. C., Lopez-Lefebvre, L. R., Rivero, R. M., Ruiz, J. M., and Romero, L. (2000).** Phenolic compounds and oxidative metabolism in green bean plants under nitrogen toxicity. *Australian journal plant physiology*. 27: 973-978.

**Sass-Kiss, A., Kiss, J., Milotay, P., Kerek, M. M., and Toth-Markus, M. (2005).** Differences in an anthocyanin and carotenoid content of fruits and vegetables. *Food research international*. 38: 1023-1029.

**Schiliro, E., Predieri, S., and Bertaccini, A. (2001).** Use of Random Amplified Polymorphic DNA analysis to detect Genetic Variation in *Pyrus* species. *Plant molecular biology reporter*. 19: 271.

**Shufflebottom, D., Edwards, K., Schuch, W., and Bevan, M. (1993).** Transcription of two members of a gene family encoding phenylalanine ammonia-lyase leads to remarkably different cell specificities and induction patterns. *The plant journal*. 3(6): 835-845.

**Skylas, D. J., Van Dyk, D., and Wrigley, C.W. (2005).** Proteomics of wheat grain. *Journal of Cereal Science*. 41: 165-179.

**Steyn, W. J., Wand S. J. E., Holcroft, D. M., and Jacobs, G. (2004).** Regulation of pear color development in relation to activity of flavonoid enzymes. *Journal of American Horticultural science*. 129 (1): 6-12.

**Steyn, W. J., Wand, S. J. E., and Holcroft, D. M. (2005).** Red colour development and loss in pears. *Acta Horticulturae*. 671: 79.

**Steyn, W. J., Wand, S. J. E., Holcroft, D. M., and Jacobs G. (2002).** Anthocyanins in vegetative tissues: a proposed unified function in photoprotection. *New Phytologist*. 155: 349-361.

**Stintzing, F. C., and Carle, R. (2004).** Functional properties of anthocyanins and betalains in plants, food and in human nutrition. *Trends in food science and technology*. 15: 19-38.

**Sullivan, J. (1998).** Anthocyanin. *International carnivorous plant society*. 1: 1.

**Takos, A. M., Jaffe, F. W., Jacob, S. R., Bogs, J., Robinson, S. P., and Walker, A. R. (2006).** Light-Induced expression of a MYB gene regulates anthocyanin biosynthesis in red apples. *Plant physiology*. 142: 1216-1232.

**Tromp, J., Webster, A. D., and Wertheim, S. J. (2005).** Fundamentals of temperate zone tree fruit production. First edition. Backhuys publishers. Netherlands. p238.

**Ubi, B. E. (2004).** External stimulation of anthocyanin biosynthesis in apple fruit. *Food, Agriculture and Environment*. 2(2): 65-70.

**Ubi, B. E. (2004).** The genetics of anthocyanin reddening in apple fruit skin. *Food, Agriculture and Environment*. 2(1): 163-165.

**Ubi, B. E., Honda, C., Bessho, H., Kondo, S., Wada, M., Kobayashi, S., and Moriguchi, T. (2006).** Expression analysis of anthocyanin biosynthetic genes in apple skin: Effect of UV-B and temperature. *Plant science*. 170: 571-578.

**van Wijk, K. J. (2001).** Challenges and Prospects of plant proteomics. *Plant physiology*. 126:501-508.

**von Neuhoff, N., and Pich, A. (2005).** Mass spectrometry-based methods for biomarker detection and analysis. *Drug discovery today: technologies.* 2(4): 361.

**Wang, H., Arakawa, O., Motomura, Y. (2000).** Influence of maturity and bagging on the relationship between anthocyanin accumulation and phenylalanine ammonia-lyase (PAL) activity in 'Jonathan' apples. *Postharvest biology and technology.* 19: 123-128.

**Wang, W., Vinocur, B., and Altman, A. (2003).** The plant response to drought, salinity and extreme temperatures: towards genetic engineering for stress tolerance. *Planta.* 218: 1-14.

**Winkel-Shirley, B., (2002).** Biosynthesis of flavonoids and effects of stress. *Current opinion in plant biology.* 5: 218-223.

**Wrolstad, R. E., Durs, R. W., and Lee, J. (2005).** Tracking colour and pigment changes in anthocyanin products. *Trends in food science and technology.* 16: 423-428.

**Wunsch, A., and Hormaza, J. I. (2007).** Characterization of variability and genetic similarity of European pear using microsatellite loci development in apple. *Scientia Horticulturae.* 113: 37-43.

**Xu, C., Garrett, W. M., Sullivan, J., Caperna, T. J., and Natarajan, S. (2006).** Separation and identification of soybean leaf proteins by two-dimensional gel electrophoresis and mass spectrometry. *Phytochemistry.* 67: 2431-2440.

**Yu, O., Matsuno, M., and Subramanian, S. (2006).** Flavonoid Compounds in Flowers: genetics and Biochemistry. *Floriculture, ornamental and plant biotechnology.* 1: 1.

**Zhang, L., Rui, Q., and Xu, L. (2005).** Degradation of the large subunit of Ribulose-1,5-Bisphosphate Carboxylase/Oxygenase in wheat leaves. *Journal of Integrative Plant Biology.* 47(1): 60-66.

**Zuo, X., and Speicher, D. W. (2000).** A method for global analysis of complex proteomes using sample prefractionation by solution isoelectrofocusing prior to two-dimensional electrophoresis. *Analytical Biochemistry*. 284: 266.



UNIVERSITY *of the*  
WESTERN CAPE